CHAPTER-1

INTRODUCTION

Non-renewable sources such as fossil fuel and renewable energy sources such as solar photovoltaic (PV) and wind are primarily used for electricity generation worldwide. The nonrenewable energy sources being of rapid depletion and their tendency to release greenhouse gases to the atmosphere have accelerated the global warming calamity. This being the case, the renewable energy sources (RESs) are of inevitable choice since they are inexhaustible and have less adverse impacts on the environment [1]. However, the main drawback of the RESs for power generation is their incapability to ensure reliability due to their operating nature that depends on weather conditions [2]. In Tanzania rural areas there is high demand of energy whereby the main energy consumption of about 88% is biomass in the form of firewood and charcoal. Increasing electricity access to at least 75% by 2033 has been the goal in the Tanzania's Rural Electrification Program of 2013-2022 [3]. To precisely achieve this goal in the Tanzanian rural areas, effective extraction of the RESs, which are enormously available, is inexorable [4]. There has currently been high promotion of off-grid solar PV and wind systems all over the world [5]. However, the inability of these sources to deliver continuous energy has made the use of energy storage system (ESS) unavoidable in order to satisfy the power demands. Hybrid solar PV and wind energy systems allow them to complement each other. It is desired that this ESS to be reduced in size due to the cost implications it can result in such hybrid power system [6]. This can be realized by integrating the renewable energy sources to form a hybrid RESs power system with battery ESS (BESS) in place [2], [6]. The BESS being a crucial component of the hybrid RESs power system, it is necessary to accurately model and determine the optimal size of the BESS due to its high investment costs. The optimal BESS sizing is to be performed since undersized BESS might not give the preferred benefits and oversized BESS leads to high capital costs of the entire power system. Hence, to effectively reduce the cost of the hybrid power system with ESS, it is imperative to optimize the size of the ESS [7], [8]. In various literature, the control approaches of hybrid RESs have been reported. Reference [9] shows analysis of the stability of hybrid solar PV power generation integrated with a battery system. Frequently, in isolated hybrid power generation systems, the voltage and frequency are controlled by appropriate switching of power converters. Authors in [10], and [11], revealed that the commonly preferred strategy in achieving frequency regulation is droop control. In relation to [12], the droop control experiences several weaknesses, such as

requirement of complex inner multi-loop feedback control, deviation of voltage and frequency at the AC bus on the loss of one of the RES. In conjunction with the RES's, ESS is being used to smooth the intermittent generation of these RES's and obtain a dispatchable output as explicated in [13], [14] and [15]. Reference [16] proposed an analytical method to find the most profitable rating of the ESS that is installed in wind farms. Similarly, in [17] sizing of ESS is considered in photovoltaic-energy storage for autonomous small islands to minimize the overall system cost. In [18], numerous optimization methods are investigated for the microgrids system including heuristic methods such as particle swarm, genetic algorithm and game theory. Furthermore, in [8], there is a grid connected microgrid in which the employed ESS is optimized in order to reduce the overall planning cost of the system. Here the mixed-integer linear programming (MILP) optimization method is used. Moreover, [19] added a reliability constraint that is responsible to limit the loss of load expectation to a certain value. In this paper, modelling and coordination control of hybrid solar PV-wind system together with battery optimization method is proposed. The control strategy involves the DC bus control through a bidirectional buck-boost converter and Point of Common Coupling (PCC) control through an inverter. The DC bus control is done to maintain voltage at the DC bus constant by charging and discharging the battery through a bidirectional DC-DC converter. On the other hand, inverter is controlled so as to maintain the voltage and the system frequency at the PCC constant. Moreover, the use of proper Maximum Power Point Tracking (MPPT) algorithm is inevitable in order to capture the maximum possible power at any instant from the solar PV generator.

CHAPTER-2

LITERATURE SURVEY

With the development of new technologies in the field of renewable energy and batteries, increasing number of houses have been equipped with renewable energy sources (RES) and energy storage systems (ESS) to reduce home energy cost. These houses usually have home energy management systems (HEMS) to control and schedule every electrical device. Various studies have been conducted on HEMS and optimization algorithms for energy cost and peak-to-average ratio (PAR) reduction. However, none of papers give a sufficient study on the utilization of main grid's electricity and selling electricity. In this paper, firstly, we propose a new HEMS architecture with RES and ESS where we take utilization of the electricity of the main grid and electricity selling into account. With the proposed HEMS, we build general mathematical formulas for energy cost and PAR during a day. We then optimize these formulas using both the particle swarm optimization (PSO) and the binary particle swarm optimization (BPSO). Results clearly show that, with our HEMS system, RES and ESS can help to drop home energy cost significantly to 19.7%, compared with the results of previous works. By increasing charge/discharge rate of ESS, energy cost can be decreased by 4.3% for 0.6 kW and 8.5% for 0.9 kW. Moreover, by using multi-objective optimization, our system can achieve better PAR with an acceptable energy cost

[1] H. T. Dinh, J. Yun, D. M. Kim, K. Lee, and D. Kim, ''A home energy management system with renewable energy and energy storage utilizing main grid and electricity selling,'' IEEE Access, vol. 8, pp. 49436–49450, 2020.

[2] C. Byers and A. Botterud, ''Additional capacity value from synergy of variable renewable energy and energy storage,'' IEEE Trans. Sustain. Energy, vol. 11, no. 2, pp. 1106–1109, Apr. 2020.

Current capacity markets often consider capacity credits from each resource independently, irrespective of the portfolio of resources, potentially overvaluing or undervaluing the capacity contribution of variable renewable energy (VRE) and energy storage (ES) in the grid. We propose a method for calculating the standalone and integrated capacity value of an added VRE resource with existing ES resources. The difference between the integrated and standalone value is the portfolio effect. This is the additional capacity value gained by the synergy of VRE and the existing fleet. Using chronological dispatch simulations and two different reliability

metrics to estimate firm capacity, we demonstrate on a small test system that the portfolio effect can be substantial.

[3] M. Rizwan, L. Hong, W. Muhammad, S. W. Azeem, and Y. Li, ''Hybrid Harris Hawks optimizer for integration of renewable energy sources considering stochastic behavior of energy sources,'' Int. Trans. Elect. Energy Syst., vol. 31, no. 2, 2021, Art. no. e12694, doi: 10.1002/2050- 7038.12694.

Renewable energy sources powered distributed generation (RES-DG) is getting more indispensable to encounter the considerable increase in demand for electric energy owing to its techno-economic benefits and eco-friendly nature. An economic solution to this demand can only be obtained with the optimal placement and sizing of RES-DGs. The optimal siting and sizing of RES-DG, such as Photovoltaic (PV) and Wind Turbine (WT) is still a hot topic due to the uncertainties in solar irradiance (SI) and wind speed (WS). The main objective of this research paper is to develop a RES-DG siting and sizing strategy for the discrete, nonlinear siting and sizing pattern of RES-DGs using a novel hybrid Harris' Hawk optimizer (HHHO), considering the stochastic nature of SI and WS. The Weibull and Beta probability density functions (PDFs) are utilized for modeling the stochastic nature of WS and SI, respectively. The optimization of the multiobjective function comprises active power loss reduction, enhancement in voltage profile, and improvement in voltage stability index (VSI). Different scenarios of single and multiple RES-DGs and capacitor banks (CB) are examined to validate the efficiency of the proposed novel HHHO based RES-DGs siting and sizing strategy. The results show a considerable reduction in power loss, enhancement in the system voltage profile, and improvement in VSI. Evaluation of results by comparing withstate-of-art hybrid algorithms shows that the proposed solution using HHHO algorithm is globally optimum.

[4] Y. Sun, Z. Zhao, M. Yang, D. Jia, W. Pei, and B. Xu, ''Overview of energy storage in renewable energy power fluctuation mitigation,'' CSEE J. Power Energy Syst., vol. 6, no. 1, pp. 160–173, 2020.

The integration of renewable energy, such as PV and wind power, has exerted great impacts on the power system with its rapid development. If the corresponding energy storage system is configured, the power system could be able to hold a higher proportion of renewable energy. Focusing on energy storage application for the output fluctuation mitigation of renewable energy, this paper first analyses the reason for renewable energy power fluctuation mitigation from the four aspects of frequency, unit ramp, low frequency oscillation and cascading failure.

In addition, the fluctuation rate standard of grid-connected renewable energy, the energy storage type and the mitigation topology are introduced. Then a summary and analysis on mitigation strategy and hybrid energy storage allocation strategy are presented. Finally, the demonstration application and development trend of energy storage are analyzed to provide reference for the promotion of energy storage in renewable energy.

[5] T. Salameh, M. A. Abdelkareem, A. G. Olabi, E. T. Sayed, M. Al-Chaderchi, and H. Rezk, ''Integrated standalone hybrid solar PV, fuel cell and diesel generator power system for battery or supercapacitor storage systems in khorfakkan, united arab emirates,'' Int. J. Hydrogen Energy, vol. 46, no. 8, pp. 6014–6027, Jan. 2021.

Renewable energy resources play a very important rule these days to assist the conventional energy systems for doing its function in the UAE due to high greenhouse gas (GHG) emissions and energy demand. In this paper, the analysis and performance of integrated standalone hybrid solar PV, fuel cell and diesel generator power system with battery energy storage system (BESS) or supercapacitor energy storage system (SCESS) in Khorfakkan city, Sharjah were presented. HOMER Pro software was used to model and simulate the hybrid energy system (HES) based on the daily energy consumption for Khorfakkan city. The simulation results show that using SCESS as an energy storage system will help the performance of HES based on the Levelized cost of energy (LCOE) and greenhouse gas (GHG) emissions. The HES with SCESS has renewable fraction (68.1%) and 0.346 $/kWh LCOE. The HES meets the annual AC primary load of the city (13.6 GWh) with negligible electricity excess and with an unmet electrical load of 1.38%. The reduction in GHG emissions for HES with SCESS was 83.2%, equivalent to saving 814,428 gallons of diesel.

[6] M. Çolak and Ä. Kaya, ''Multi-criteria evaluation of energy storage technologies based on hesitant fuzzy information: A case study for turkey,'' J. Energy Storage, vol. 28, Apr. 2020, Art. no. 101211.

Energy storage technologies (ESTs) enable to cope with intermittency of energy sources by storing excess energy to use when it is needed. Therefore, evaluation of energy storage alternatives (or technologies) is completely critical and can be exactly considered as a multi-criteria decision making (MCDM) problem. It is clear that we have to evaluate this problem in terms of both qualitative and quantitative criteria. We should also take into account decision makers' linguistic evaluations and their experiences. At this point, the fuzzy set theory (FST) that is an effective tool to utilize from human judgments and linguistic evaluations in the

decision making process can be successfully used. Hesitant fuzzy sets (HFSs) that enable to have several membership values between 0 and 1 for an element of the set can be used for this aim as an extension of ordinary fuzzy sets. In this paper, an integrated MCDM model consists of Delphi, Analytic Hierarchy Process (AHP) and VIsekriterijumska Optimizcija I Kompromisno Resenje (VIKOR) methods has been proposed to evaluate EST alternatives for Turkey under hesitant fuzzy environment. For this aim, a hierarchical decision model consisting of four main criteria and nineteen sub-criteria with nine EST alternatives has been constructed. While hesitant fuzzy AHP (HF-AHP) method has been utilized to determine weights of criteria, the alternatives have been ranked by using hesitant fuzzy VIKOR (HF-VIKOR) method. A sensitivity analysis based on change of some parameters has been also performed to analyze the obtained results and to demonstrate sensitiveness of the proposed MCDM model. A comparative analysis has been also realized to confirm the validity of the proposed fuzzy based methodology. For this aim, hesitant fuzzy Technique for Order Preference by Similarity to Ideal Solution (HF-TOPSIS) method has been applied as another distance-based methodology. One of the obtained results of this study is that the criteria economic and technical have been determined as the most and the least important main criteria and the weights of them have been achieved as 0.342 and 0.203, respectively. Additionally, the alternative EST named "Compressed Air" has been determined as the most suitable energy storage technology alternative for Turkey.

[7] M. A. Hannan, M. M. Hoque, A. Mohamed, and A. Ayob, ''Review of energy storage systems for electric vehicle applications: Issues and challenges,'' Renew. Sustain. Energy Rev., vol. 69, pp. 771–789, Mar. 2017.

The electric vehicle (EV) technology addresses the issue of the reduction of carbon and greenhouse gas emissions. The concept of EVs focuses on the utilization of alternative energy resources. However, EV systems currently face challenges in energy storage systems (ESSs) with regard to their safety, size, cost, and overall management issues. In addition, hybridization of ESSs with advanced power electronic technologies has a significant influence on optimal power utilization to lead advanced EV technologies. This paper comprehensively reviews technologies of ESSs, its classifications, characteristics, constructions, electricity conversion, and evaluation processes with advantages and disadvantages for EV applications. Moreover, this paper discusses various classifications of ESS according to their energy formations, composition materials, and techniques on average power delivery over its capacity and overall efficiencies exhibited within their life expectancies. The rigorous review indicates

that existing technologies for ESS can be used for EVs, but the optimum use of ESSs for efficient EV energy storage applications has not yet been achieved. This review highlights many factors, challenges, and problems for sustainable development of ESS technologies in next-generation EV applications. Thus, this review will widen the effort toward the development of economic and efficient ESSs with a longer lifetime for future EV uses.

[8] R. Amirante, E. Cassone, E. Distaso, and P. Tamburrano, ''Overview on recent developments in energy storage: Mechanical, electrochemical and hydrogen technologies,'' Energy Convers. Manage., vol. 132, pp. 372–387, Jan. 2017

Energy production is changing in the world because of the need to reduce greenhouse gas emissions, to reduce the dependence on carbon/fossil sources and to introduce renewable energy sources. Despite the great amount of scientific efforts, great care to energy storage systems is necessary to overcome the discontinuity in the renewable production. A wide variety of options and complex characteristic matrices make it difficult and so in this paper the authors show a clear picture of the available state-of-the-art technologies. The paper provides an overview of mechanical, electrochemical and hydrogen technologies, explaining operation principles, performing technical and economic features. Finally a schematic comparison among the potential utilizations of energy storage systems is presented.

CHAPTER-3

PHOTOVOLTAIC TECHNOLOGY

Photovoltaic's is the field of technology and research related to the devices which directly convert sunlight into electricity using semiconductors that exhibit the photovoltaic effect. Photovoltaic effect involves the creation of voltage in a material upon exposure to electromagnetic radiation.

The photovoltaic effect was first noted by a French physicist, Edmund Becquerel, in 1839, who found that certain materials would produce small amounts of electric current when exposed to light. In 1905, Albert Einstein described the nature of light and the photoelectric effect on which photovoltaic technology is based, for which he later won a Nobel prize in physics. The first photovoltaic module was built by Bell Laboratories in 1954. It was billed as a solar battery and was mostly just a curiosity as it was too expensive to gain widespread use. In the 1960s, the space industry began to make the first serious use of the technology to provide power aboard spacecraft. Through the space programs, the technology advanced, its reliability was established, and the cost began to decline. During the energy crisis in the 1970s, photovoltaic technology gained recognition as a source of power for non-space applications.

The solar cell is the elementary building block of the photovoltaic technology. Solar cells are made of semiconductor materials, such as silicon. One of the properties of semiconductors that makes them most useful is that their conductivity may easily be modified by introducing impurities into their crystal lattice. For instance, in the fabrication of a photovoltaic solar cell, silicon, which has four valence electrons, is treated to increase its conductivity. On one side of the cell, the impurities, which are phosphorus atoms with five valence electrons (n-donor), donate weakly bound valence electrons to the silicon material, creating excess negative charge carriers.

On the other side, atoms of boron with three valence electrons (p-donor) create a greater affinity than silicon to attract electrons. Because the p-type silicon is in intimate contact with the n-type silicon a p-n junction is established and a diffusion of electrons occurs from the region of high electron concentration (the n-type side) into the region of low electron concentration (p-type side). When the electrons diffuse across the p-n junction, they recombine with holes on the p-type side.However, the diffusion of carriers does not occur indefinitely, because the imbalance

of charge immediately on either sides of the junction originates an electric field. This electric field forms a diode that promotes current to flow in only one direction.

Ohmic metal-semiconductor contacts are made to both the n-type and p-type sides of the solar cell, and the electrodes are ready to be connected to an external load. When photons of light fall on the cell, they transfer their energy to the charge carriers. The electric field across the junction separates photo-generated positive charge carriers (holes) from their negative counterpart (electrons). In this way an electrical current is extracted once the circuit is closed on an external load.

3.1 Solar cell:

The photovoltaic effect was first reported by Edmund Becquerel in 1839when he observed that the action of light on a silver coated platinum electrode immersed in electrolyte produced an electric current. Forty years later the first solid state photovoltaic devices were constructed by workers investigating the recently discovered photoconductivity of selenium. In1876 William Adams and Richard Day found that a photocurrent could be produced in a sample of selenium when contacted by two heated platinum contacts. The photovoltaic action of the selenium differed from its photoconductive action in that a current was produced spontaneously by the action of light.

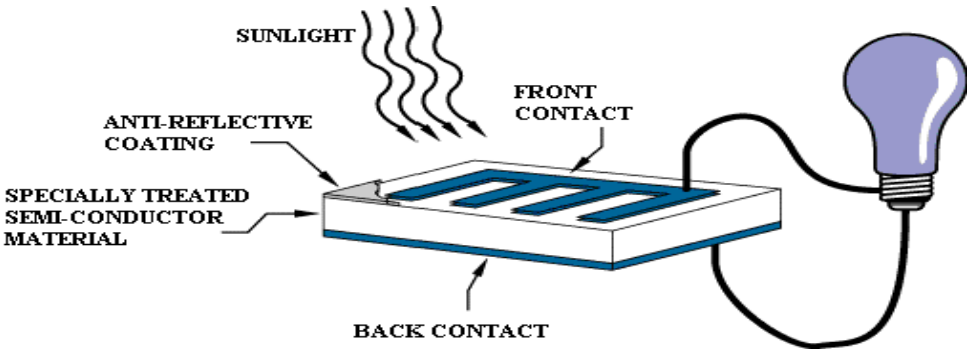

Fig 3.1: Solar cell.

No external power supply was needed. In this early photovoltaic device, a rectifying junction had been formed between the semiconductor and the metal contact. In 1894, Charles Fritts prepared what was probably the first large area solar cell by pressing a layer of selenium between gold and another metal. In the following years photovoltaic effects were observed in copper {copper oxide thin lm structures, in lead supplied and thallium supplied. These early

cells were thin film Schottky barrier devices, where a semitransparent layer of metal deposited on top of the semiconductor provided both the asymmetric electronic junction, which is necessary for photovoltaic action and access to the junction for the incident light. The photovoltaic effect of structures like this was related to the existence of a barrier to current flow at one of the semiconductor {metal interfaces (i.e., rectifying action) by Goldman and Brodsky in 1914. Later, during the 1930s, the theory of metal {semiconductor barrier layers was developed by Walter Schottky, Neville Mott and others.

However, it was not the photovoltaic properties of materials like selenium which excited researchers, but the photoconductivity. The fact that the current produced was proportional to the intensity of the incident light, and related to the wavelength in a definite way meant that photoconductive materials were ideal for photographic light meters. The photovoltaic effecting barrier structures was an added benefit, meaning that the light meter could operate without a power supply. It was not until the 1950s, with the development of good quality silicon wafers for applications in the new solid-state electronics, that potentially useful quantities of power were produced by photovoltaic devices in crystalline silicon.

In the 1950s, the development of silicon electronics followed the discovery of a way to manufacture p-n junctions in silicon. Naturally n type silicon wafers developed a p type skin when exposed to the gas boron trichloride.Part of the skin could be etched away to give access to the n type layer beneath. These p{n junction structures produced much better rectifying action than Schottky barriers, and better photovoltaic behavior. The first silicon solar cell was reported by Chapin, Fuller and Pearson in 1954 and converted sunlight with an efficiency of 6%, six times higher than the best previous attempt. That figure was to rise significantly over the following years and decades but, at an estimated production cost of some $200 per Watt, these cells were not seriously considered for power generation for several decades. Nevertheless, the early silicon solar cell did introduce the possibility of power generation in remote locations where fuel could not easily be delivered. The obvious application was to satellites where the requirement of reliability and low weight made the cost of the cells unimportant and during the 1950s and 60s, silicon solar cells were widely developed for applications in space.Also in 1954, a cadmium supplied p-n junction was produced with an efficiency of 6%, and in the following years studies of p-n junction photovoltaic devices in gallium arsenide, indium phosphate and cadmium telluride were stimulated by theoretical work indicating that these materials would offer a higher efficiency. However, silicon remained and

remains the foremost photovoltaic material, benefiting from the advances of silicon technology for the microelectronics industry. Short histories of the solar cell are given elsewhere.

In the 1970s the crisis in energy supply experienced by the oil-dependent western world led to a sudden growth of interest in alternative sources of energy, and funding for research and development in those areas. Photovoltaic's was a subject of intense interest during this period, and a range of strategies for producing photovoltaic devices and materials more cheaply and for improving device.

Efficiency was explored. Routes to lower cost included photo electrochemical junctions, and alternative materials such as polycrystalline silicon, amorphous silicon, other `thin _lm' materials and organic conductors. Strategies for higher efficiency included tandem and other multiple band gap designs. Although none of these led to widespread commercial development, our understanding of the science of photovoltaic is mainly rooted in this period.

During the 1990s, interest in photovoltaic's expanded, along with growing awareness of the need to secure sources of electricity alternative to fossil fuels. The trend coincides with the widespread deregulation of the electricity markets and growing recognition of the viability of decentralized power. During this period, the economics of photovoltaic's improved primarily through economies of scale. In the late 1990s the photovoltaic production expanded at a rate of 15{25% per annum, driving a reduction in cost. Photovoltaic first became competitive in contexts where conventional electricity supply is most expensive, for instance, for remote low power applications such as navigation, telecommunications, and rural electrification and for enhancement of supply in grid-connected loads at peak use [Anderson, 2001]. As prices fall, new markets are opened up. An important example is building integrated photovoltaic applications, where the cost of the photovoltaic system is offset by the savings in building materials.There are several types of solar cells. However, more than 90 % of the solar cells currently made worldwide consist of wafer-based silicon cells.

They are either cut from a single crystal rod or from a block composed of many crystals and are correspondingly called mono-crystalline or multi-crystalline silicon solar cells. Wafer-based silicon solar cells are approximately 200 μm thick. Another important family of solar cells is based on thin-films, which are approximately 1-2 μm thick and therefore require significantly less active, semiconducting material. Thin-film solar cells can be manufactured at lower cost in large production quantities; hence their market share will likely increase in the future. However, they indicate lower efficiencies than wafer-based silicon solar cells, which

mean that more exposure surface and material for the installation is required for a similar performance.

A number of solar cells electrically connected to each other and mounted in a single support structure or frame is called a 'photovoltaic module'. Modules are designed to supply electricity at a certain voltage, such as a common 12 volt system. The current produced is directly dependent on the intensity of light reaching the module. Several modules can be wired together to form an array. Photovoltaic modules and arrays produce direct-current electricity. They can be connected in both series and parallel electrical arrangements to produce any required voltage and current combination.

3.2 Electrical connection of the cells:

The electrical output of a single cell is dependent on the design of the device and the Semi-conductor material(s) chosen, but is usually insufficient for most applications. In order to provide the appropriate quantity of electrical power, a number of cells must be electrically connected. There are two basic connection methods: series connection, in which the top contact of each cell is connected to the back contact of the next cell in the sequence, and parallel connection, in which all the top contacts are connected together, as are all the bottom contacts. In both cases, this results in just two electrical connection points for the group of cells.

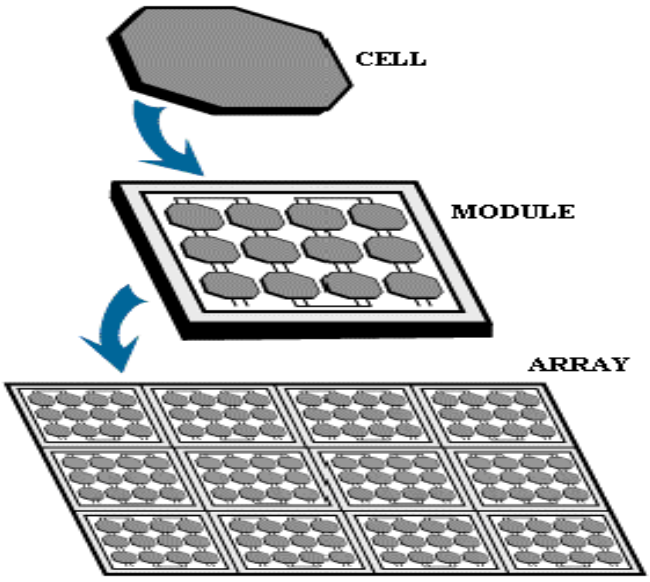

Fig 3.2.1: cell, module and array

➢ Series connection:

Figure shows the series connection of three individual cells as an example and the resultant group of connected cells is commonly referred to as a series string.

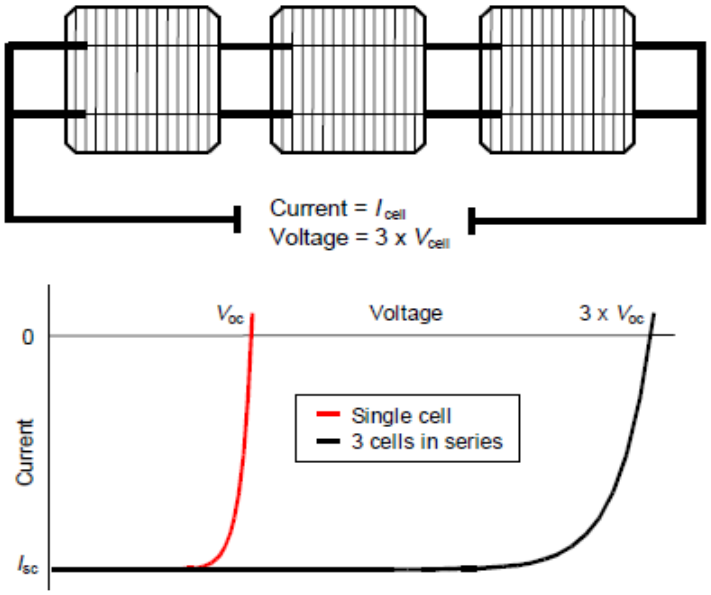

Fig. 3.2.2: Series connection of cells, with resulting current–voltage characteristic

The current output of the string is equivalent to the current of a single cell, but the voltage output is increased, being an addition of the voltages from all the cells in the string (i.e. in this case, the voltage output is equal to 3Vcell).It is important to have well matched cells in the series string, particularly with respect to current. If one cell produces a significantly lower current than the other cells (under the same illumination conditions), then the string will operate at that lower current level and the remaining cells will not be operating at their maximum power points.

➢ Parallel connection:

Figure shows the parallel connection of three individual cells as an example. In this case, the current from the cell group is equivalent to the addition of the current from each cell (in this case, 3 I cell), but the voltage remains equivalent to that of a single cell.

As before, it is important to have the cells well matched in order to gain maximum output, but this time the voltage is the important parameter since all cells must be at the same operating

voltage. If the voltage at the maximum power point is substantially different for one of the cells, then this will force all the cells to operate off their maximum power point, with the poorer cell being pushed towards its open-circuit voltage value and the better cells to voltages below the maximum power point voltage. In all cases, the power level will be reduced below the optimum.

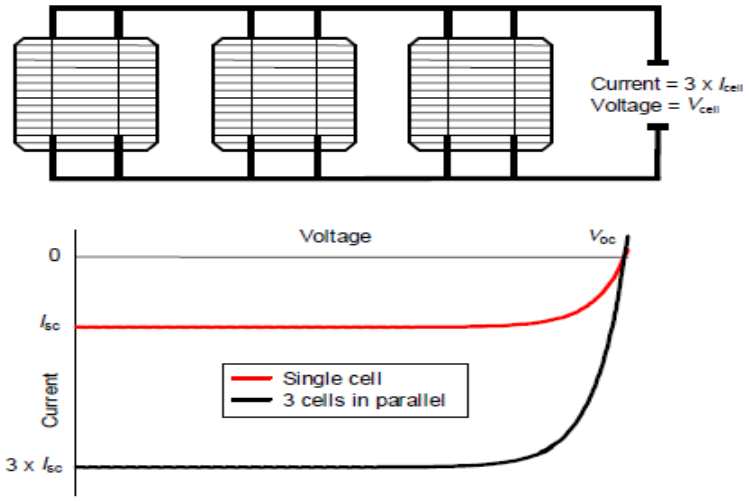

Fig.3.2.3: Parallel connection of cells, with resulting current–voltage characteristic

3.3 The photovoltaic array:

A PV array consists of a number of PV modules, mounted in the same plane and electrically connected to give the required electrical output for the application. The PV array can be of any size from a few hundred watts to hundreds of kilowatts, although the larger systems are often divided into several electrically independent sub arrays each feeding into their own power conditioning system.

3.4 The photovoltaic system:

A PV system consists of a number of interconnected components designed to accomplish a desired task, which may be to feed electricity into the main distribution grid, to pump water from a well, to power a small calculator or one of many more possible uses of solar-generated electricity. The design of the system depends on the task it must perform and the location and other site conditions under which it must operate. This section will consider the components of a PV system, variations in design according to the purpose of the system, system sizing and aspects of system operation and maintenance.

3.4.1 System design:

There are two main system configurations – stand-alone and grid-connected. As its name implies, the stand-alone PV system operates independently of any other power supply and it usually supplies electricity to a dedicated load or loads. It may include a storage facility (e.g. battery bank) to allow electricity to be provided during the night or at times of poor sunlight levels. Stand-alone systems are also often referred to as autonomous systems since their operation is independent of other power sources. By contrast, the grid-connected PV system operates in parallel with the conventional electricity distribution system. It can be used to feed electricity into the grid distribution system or to power loads which can also be fed from the grid.

It is also possible to add one or more alternative power supplies (e.g. diesel generator, wind turbine) to the system to meet some of the load requirements. These systems are then known as 'hybrid' systems.

Hybrid systems can be used in both stand-alone and grid-connected applications but are more common in the former because, provided the power supplies have been chosen to be complementary, they allow reduction of the storage requirement without increased loss of load probability. Figures below illustrate the schematic diagrams of the three main system types.

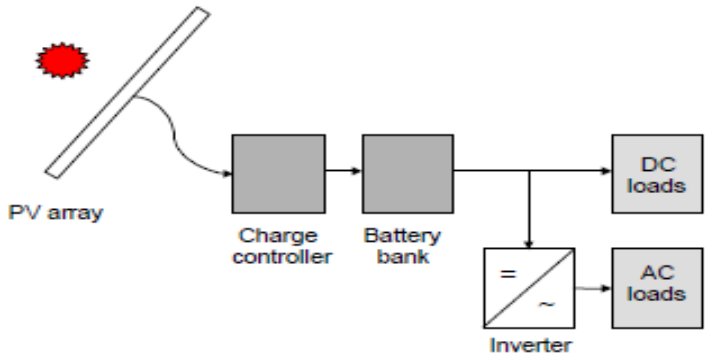

Fig.3.4.1: Schematic diagram of a stand-alone photovoltaic system.

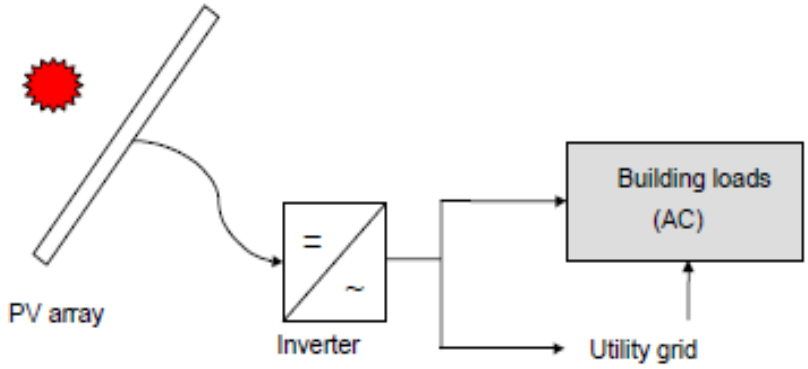

Fig.3.4.2: Schematic diagram of grid-connected photovoltaic system.

CHAPTER 4

DC-DC CONVERTERS

4.1 Introduction:

A DC–DC Converter with a high step-up voltage gain is used for many applications such as high-intensity discharge lamp ballasts for Automobile headlamps, Fuel Cell Energy Conversion systems, Solar Cell Energy Conversion systems and Battery backup systems for Uninterruptible Power Supplies. Theoretically, a DC–DC Boost Converter can achieve a high step-up voltage gain with an extremely high duty ratio. However, in practice, the step-up voltage gain is limited due to the effect of power switches, rectifier diodes and the equivalent series resistance of inductors and capacitors.

In general, a Conventional Boost Converter can be adopted to provide a high step-up voltage gain with a large duty ratio. However, the Conversion efficiency and the step-up voltage gain are limited due to the constraints of the losses of power switches and diodes, the equivalent series resistance of inductors and capacitors and the reverse recovery problem of diodes. However, the active switch of these converters will suffer very high voltage stress and high power dissipation due to the leakage inductance of the transformer.

To reduce the voltage spike, a resistor–capacitor–diode snubber can be employed to limit the voltage stress on the active switch. However, the efficiency will be reduced. High step-up converters with a low input current ripple based on the coupled inductor have been developed. The low input current ripple of these converters is realized by using an additional LC circuit with a coupled inductor.

However, leakage inductance issues that relate to the Voltage Spike and efficiency remain significant. An integrated Boost–fly back converter based on a coupled inductor with high efficiency and high step-up voltage gain has been presented. The energy stored in the leakage inductor is recycled into the output during the switch off period. Thus, the efficiency can be increased and the voltage stress on the active switch can be suppressed. Many step-up converters, which use an output voltage stacking to increase the voltage gain, are presented.

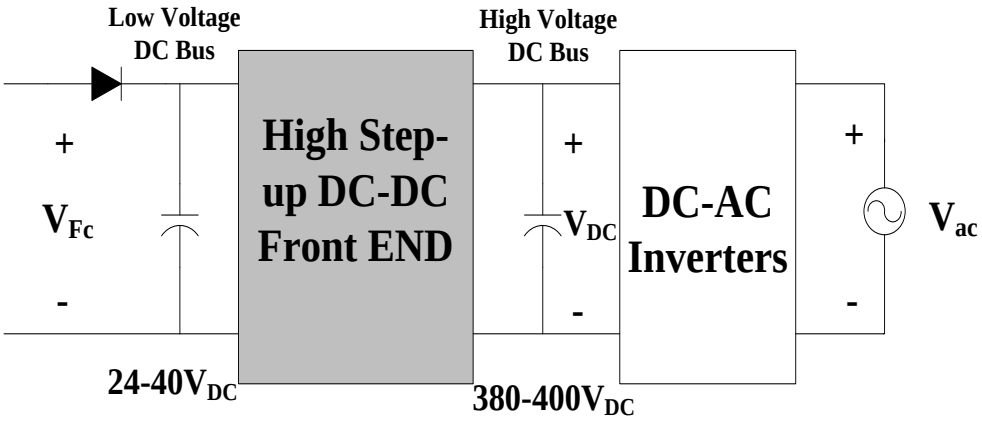

Figure 4.1: General Power generation system with a high step-up converter

A high step-up DC–DC Converter is shown in Figure 4.1 with an integrated coupled inductor and a common mode electromagnetic interference reduction filter. Here a Step up-fly back converter with a coupled inductor and an output voltage stacking is developed. A high step-up converter, which utilizes a coupled inductor and a voltage doubler technique on the output voltage stacking to achieve a high step-up voltage gain, is introduced. A high step-up boost converter that uses multiple coupled inductors for the output voltage stacking is proposed.

Additionally, step-up converters, which use a voltage lift, are introduced. Since the switch must suffer high current during the switch on period, this technique is appropriate for low-output-power applications. Since the low voltage rating and the low conducting resistance R_{DS} (on) of the power switch are used for these converters, the high conversion efficiency can be achieved. However, the requirement for a coupled inductor with a high coupling coefficient will result in manufacturing difficulty and cost increment. A high step-up converter, which uses a three state switching cell and a voltage multiplier stage based on capacitors, can achieve high step-up gain.

The Power engineering is the method used to supply electrical energy from a source to its users. It is of vital importance to industry. It is likely that the air we breathe and water we drink are taken for granted until they are not there. Energy conversion technique is the main focus of power engineering.

The corresponding equipment can be divided into four groups:

- AC/AC transformers
- AC/DC rectifiers
- DC/DC converters
- DC/AC inverters

The Grid interconnection of PV/Fuel Cell system requires power converters to meet the grid requirements like Voltage amplitude, frequency and phase angle. First convert the low voltage dc into high voltage dc by using boost dc-dc converter and then convert this dc voltage into ac by using inverters and finally connect the whole system to grid. This type of system i.e., dc-dc and dc-ac conversion is called two stage conversion system.

The DC-DC converters are electronic devices used whenever we want to change DC electrical power efficiently from one voltage level to another. They are needed because unlike AC, DC cannot simply be stepped up or down using a transformer. In many ways, a DC-DC converter is the equivalent of a transformer.

The dc-dc converters can be viewed as dc transformer that delivers a dc voltage or current at a different level than the input source. Electronic switching performs this dc transformation as in conventional transformers and not by electromagnetic means. The dc-dc converters find wide applications in regulated switch-mode dc power supplies and in dc motor drive applications.

The DC-DC converters are non-linear in nature. The design of high performance control for them is a challenge for both the control engineering engineers and power electronics engineers. In general, a good control for dc-dc converter always ensures stability in arbitrary operating condition. Moreover, good response in terms of rejection of load variations, input voltage changes and even parameter uncertainties is also required for a typical control scheme.

After pioneer study of dc-dc converters, a great deal of efforts has been directed in developing the modelling and control techniques of various dc-dc converters. Classic linear approach relies on the state averaging techniques to obtain the state-space averaged equations. From the state-space averaged model, possible perturbations are introduced into the state variables around the operating point. On the basis of the equations, transfer functions of the open-loop plant can be obtained. A linear controller is easy to be designed with these necessary transfer functions based on the transfer function.

The DC to DC converters are important in portable electronic devices such as cellular phones and laptop computers, which are supplied with power from batteries primarily. Such electronic devices often contain several sub-circuits, each with its own voltage level requirement different than that supplied by the battery or an external supply i.e., sometimes higher or lower than the supply voltage and possibly even negative voltage. Additionally, the battery voltage declines as its stored power is drained. Switched DC to DC converters

offer a method to increase voltage from a partially lowered battery voltage thereby saving space instead of using multiple batteries to accomplish the same thing.

DC-DC converters are electronic devices that are used whenever we want to change DC electrical power efficiently from one voltage level to another. Generically speaking the use of a switch or switches for the purpose of power conversion can be regarded as a SMPS. From now onwards whenever we mention DC-DC Converters we shall address them with respect to SMPS.

A few applications of interest of DC-DC converters are where 5V DC on a personal computer motherboard must be stepped down to 3V, 2V or less for one of the latest CPU chips; where 1.5V from a single cell must be stepped up to 5V or more, to operate electronic circuitry. In all of these applications, we want to change the DC energy from one voltage level to another, while wasting as little as possible in the process. In other words, we want to perform the conversion with the highest possible efficiency.

4.2 Types of DC-DC Converters:

There are many different types of DC-DC converters, each of which tends to be more suitable for some type of applications than for others. For convenience they can be classified into various groups. However, for example some converters are only suitable for stepping down the voltage, while others are only suitable for stepping it up and a third group can be used for either. Here we are going to see main types of DC-DC converters.

Currently DC-DC converters can be divided into two types as follows.

- Non-isolated dc-dc converters
- Isolated dc-dc converters

4.3 Non-isolated DC-DC Converters:

The non-isolated converter usually employs an inductor and there is no dc voltage isolation between the input and the output. The vast majority of applications do not require dc isolation between its input and output voltages. The non-isolated dc-dc converter has a dc path between its input and output. Battery-based systems that don’t use the ac power line represent a major application for non-isolated dc-dc converters. Point-of-load dc-dc converters that draw input power from an isolated dc-dc converter, such as a bus converter represent another widely used non-isolated application.Most of these dc-dc converter ICs use either an internal or external synchronous rectifier. Their only magnetic component is usually an output inductor and thus

less susceptible to generating electromagnetic interference. For the same power and voltage levels, it usually has lower cost and fewer components while requiring less pc-board area than an isolated dc-dc converter. For lower voltages, non-isolated buck converters can be used.

There are five main types of converter in this non-isolating group. They are as follows.

- Buck Converter
- Boost Converter
- Buck-Boost Converter
- Cuk Converter

The Buck converter is used for voltage step-down reduction, while the Boost converter is used for voltage step-up. The Buck-Boost and Cuk converters can be used for either step-down or step-up, but are essentially voltage polarity reversers or 'inverters'. The Charge-pump converter is used for either voltage step-up or voltage inversion, but only in relatively low power applications.

4.3.1 Buck Converter:

The buck converter is the most widely used dc-dc converter topology in power Management and Microprocessor Voltage Regulator applications. Those applications require fast load and line transient responses and high efficiency over a wide load current range. They can convert a voltage source into a lower regulated voltage. For example, within a computer system, voltage needs to be stepped down and a lower voltage needs to be maintained. For this purpose the Buck Converter can be used. Furthermore, buck converters provide longer battery life for mobile systems that spend most of their time in "stand-by". Buck regulators are often used as switch-mode power supplies for base band digital core and the RF Power Amplifier.

The step-down dc-dc converter, commonly known as a buck converter, is shown in Fig.4.2(a) It consists of dc input voltage source V_S, controlled switch S, diode D, filter inductor L, filter capacitor C, and load resistance R. Typical waveforms in the converter are shown in Fig.4.2(b) under the assumption that the inductor current is always positive. The state of the converter in which the inductor current is never zero for any period of time is called the continuous conduction mode (CCM). It can be seen from the circuit that when the switch S is commanded to the on state, the diode D is reverse-biased. When the switch S is off, the diode conducts to support an uninterrupted current in the inductor. The relationship among the input voltage, output voltage, and the switch duty ratio D can be derived, for instance, from the inductor

voltage V_L waveform (see Fig. 4.2(b)). According to Faraday's law, the inductor volt-second product over a period of steady-state operation is zero.

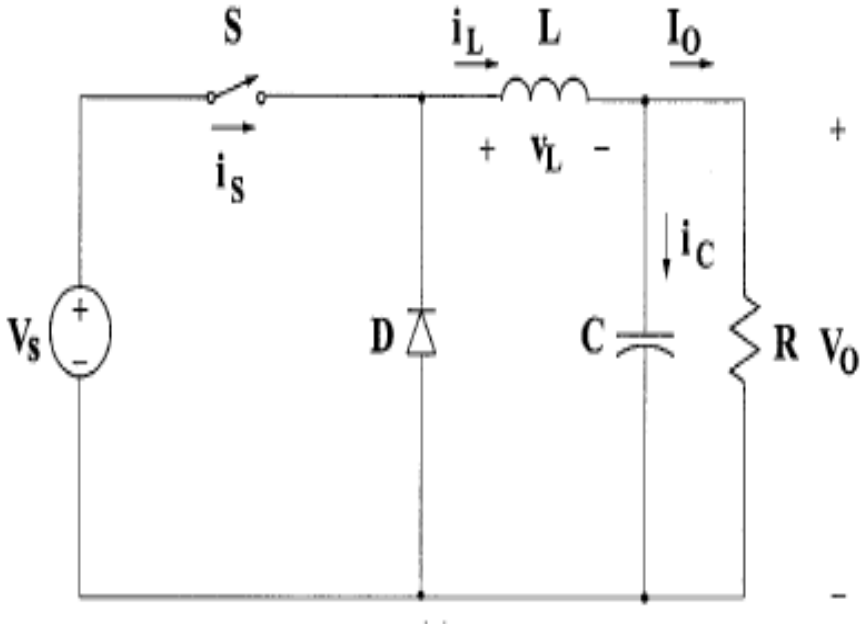

(a)

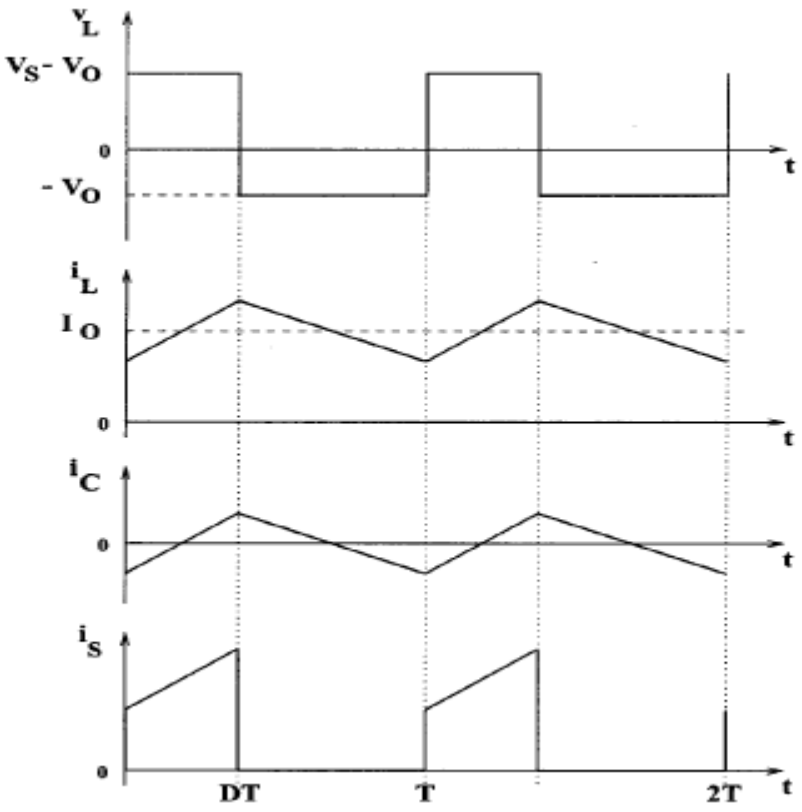

(b)

Figuree4.2 Buck converter: (a) circuit diagram; (b) waveforms.

For the buck converter

$$(V_S-V_O)DT= -V_O(1-D)T \qquad (4.1)$$

Hence, the dc voltage transfer function, defined as the ratio of the output voltage to the input voltage is

$$M_V = \frac{Vo}{Vs} = D \qquad (4.2)$$

It can be seen from Eq. (4.1) that the output voltage is always smaller that the input voltage. The dc-dc converters can operate in two distinct modes with respect to the inductor current i_L. Figure 4.2(b) depicts the CCM in which the inductor current is always greater than zero. When the average value of the output current is low (high R) and=or the switching frequency f is low, the converter may enter the discontinuous conduction mode (DCM). In the DCM, the inductor current is zero during a portion of the switching period. The CCM is preferred for high efficiency and good utilization of semiconductor switches and passive components. The DCM may be used in applications with special control requirements because the dynamic order of the converter is reduced (the energy stored in the inductor is zero at the beginning and at the end of each switching period). It is uncommon to mix these two operating modes because of different control algorithms. For the buck converter, the value of the filter inductance that determines the boundary between CCM and DCM is given by

$$L_b = \frac{(1-D)R}{2f} \qquad (4.3)$$

For typical values of D = 0.5, R=10Ω, and f =100 kHz, the boundary is L_b = 25mH. For L > L_b the converter operates in the CCM. The filter inductor current $i_L$in the CCM consists of a dc component I_O with a superimposed triangular ac component. Almost all of this ac component flows through the filter capacitor as a current i_c . Current i_c causes a small voltage ripple across the dc output voltage V_O. To limit the peak-to-peak value of the ripple voltage below a certain value Vr , the filter capacitance C must be greater than

$$C_{min} = \frac{(1-D)Vo}{(8VrLf^2)} \qquad (4.4)$$

At D = 0.5, V_r/V_O= 1%, L = 25mH, and f = 100 kHz, the minimum capacitance is Cmin .= 25 mF.

Equations (4.3) and (4.4) are the key design equations for the buck converter. The input and output dc voltages (hence, the duty ratio D), and the range of load resistances R are usually determined by preliminary specifications. The designer needs to determine values of passive components L and C, and of the switching frequency f . The value of the filter inductor L is

calculated from the CCM=DCM condition using Eq. (4.3). The value of the filter capacitor C is obtained from the voltage ripple condition Eq. (4.4). For the compactness and low conduction losses of a converter, it is desirable to use small passive components. Equations (4.3) and (4.4) show that it can be accomplished by using a high switching frequency f .The switching frequency is limited, however, by the type of semiconductor switches used and by switching losses. It should also be noted that values of L and C may be altered by the effects of parasitic components in the converter, especially by the equivalent series resistance of the capacitor.

4.3.2 Boost Converter:

A Boost Converter i.e. Step-up Converter is a DC-to-DC power converter with an output voltage greater than its input voltage. It is a class of switched mode power supply containing at least two semiconductor switches i.e., a diode and a transistor and at least one energy storage element i.e., a capacitor, inductor or the two in combination. Filters made of capacitors sometimes in combination with inductors are normally added to the output of the converter to reduce output voltage ripple.

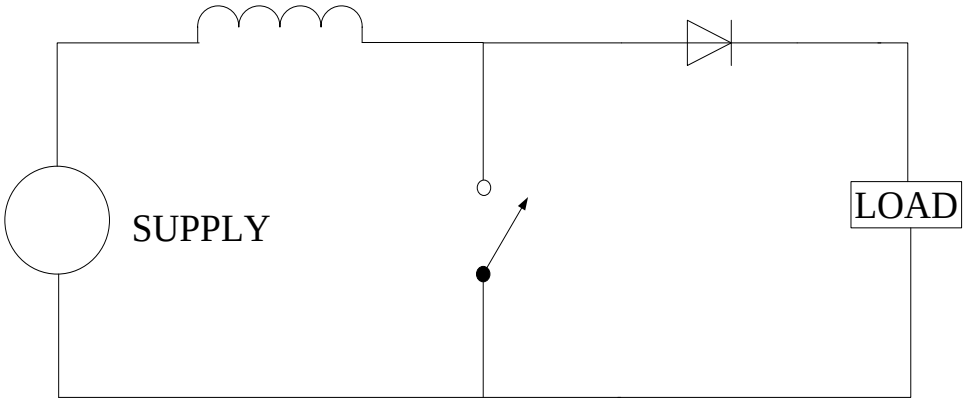

Figure 4.3: Basic schematic of a Boost Converter

4.3.2.1 Overview of Boost Converter:

Power for the Boost Converter can come from any suitable DC sources, such as batteries, solar panels, rectifiers and DC generators. A process that changes one DC voltage to a different DC voltage is called DC to DC conversion. A boost converter is a DC-to-DC converter with an output voltage greater than the source voltage. A boost converter is sometimes called a step-up converter since it “steps up” the source voltage. Since power P=VI must be conversed, the output current is lower than the source current.

4.3.2.2 History:

For high efficiency, the SMPS switch must turn on and off quickly and have low losses. The advent of a commercial semiconductor switch in the 1950s represented a major milestone that made SMPSs such as the boost converter possible. The major DC to DC converters were developed in the early 1960s when semiconductor switches had become available. The aero scope industry's need for small, lightweight and efficient power converters led to the converter's rapid development.

Switched systems such as SMPS are a challenge to design since its model depends on whether a switch is opened or closed. R. D. Middle Brook from Caltech in 1977 published the models for DC to DC converters used today. Middle Brook averaged the circuit configurations for each switch state in a technique called state-space averaging. This simplification reduced two systems into one. The new model led to insightful design equations which helped SMPS growth.

4.3.2.3 Applications:

Battery powered systems often stack cells in series to achieve higher voltage. However, sufficient stacking of cells is not possible in many high voltage applications due to lack of space. Boost converters can increase the voltage and reduce the number of cells. Two battery powered applications that use boost converters are Hybrid Electric Vehicles and lighting systems.

A boost converter is used as the voltage increase mechanism in the circuit known as the 'Joule thief'. This circuit topology is used with low power battery applications and is aimed at the ability of a boost converter to 'steal' the remaining energy in a battery. This energy would otherwise be wasted since the low voltage of a nearly depleted battery makes it unusable for a normal load. This energy would otherwise remain untapped because many applications do not allow enough current to flow through a load when voltage decreases. This voltage decrease occurs as batteries become depleted and is a characteristic of the ubiquitous alkaline battery. Since $P=V^2/R$ as well and R tends to be stable, power available to the load goes down significantly as voltage decreases.

4.3.2.4 Operating principle:

the key principle that drives the Boost Converter is the tendency of an inductor to resist changes in current. In a boost converter, the output voltage is always higher than the input voltage. A schematic of a boost power stage is shown in Figure 4.2. When the switch is closed, current flows through the inductor, which stores energy from the current in a magnetic field. During this time, the switch acts like a short circuit in parallel with the diode and the load, so no current flows to the right hand side of the circuit.

When the switch is opened, the short circuit is removed and the load is back in play in the circuit. This represents a sudden increase in the impedance of the circuit, which, by Ohm's law will demand either a decrease in current or an increase in voltage. The inductor will tend to resist such a sudden change in the current, which it does by acting as a voltage source in series with the input source, thus increasing the total voltage seen by the right hand side of the circuit and thereby preserving the current level that was seen when the switch was closed. This is done using the energy stored by the inductor. Over time, the energy stored in the inductor will discharge into the right hand side of the circuit, bringing the net voltage back down.

If the switch is cycled fast enough, the inductor will not discharge fully in between charging stages and the load will always see a voltage greater than that of the input source alone when the switch is opened. Also while the switch is opened, the capacitor in parallel with the load is charged to this combined voltage. When the switch is then closed and the right hand side is shorted out from the left hand side, the capacitor is therefore able to provide the voltage and energy to the load. During this time, the blocking diode prevents the capacitor from discharging through the switch. The switch must of course be opened again fast enough to prevent the capacitor from discharging too much.

The basic principle of a Boost Converter consists of two distinct states:

- In the On-state, the switch S is closed, resulting in an increase in the inductor current.
- In the Off-state, the switch S is open and the only path offered to inductor current is through the fly back diode D, the capacitor C and the load R. This result in transferring the energy accumulated during the On-state into the capacitor.

The input current is the same as the inductor current as can be seen in figure 4.4.So it is not discontinuous as in the buck converter and the requirements on the input filter are relaxed compared to a buck converter.

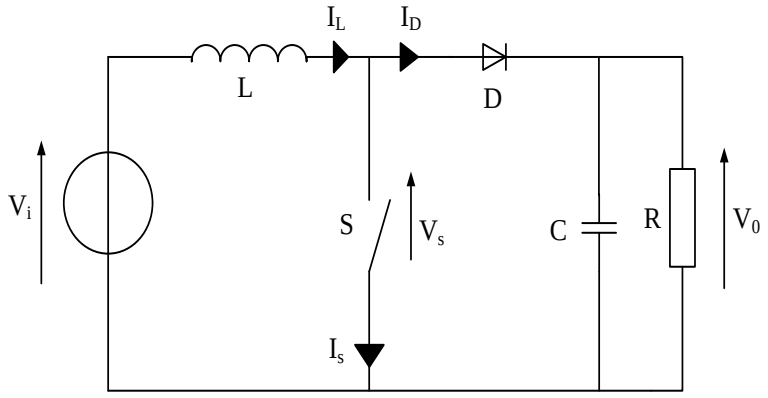

Figure 4.4: Overall diagram of Boost Converter

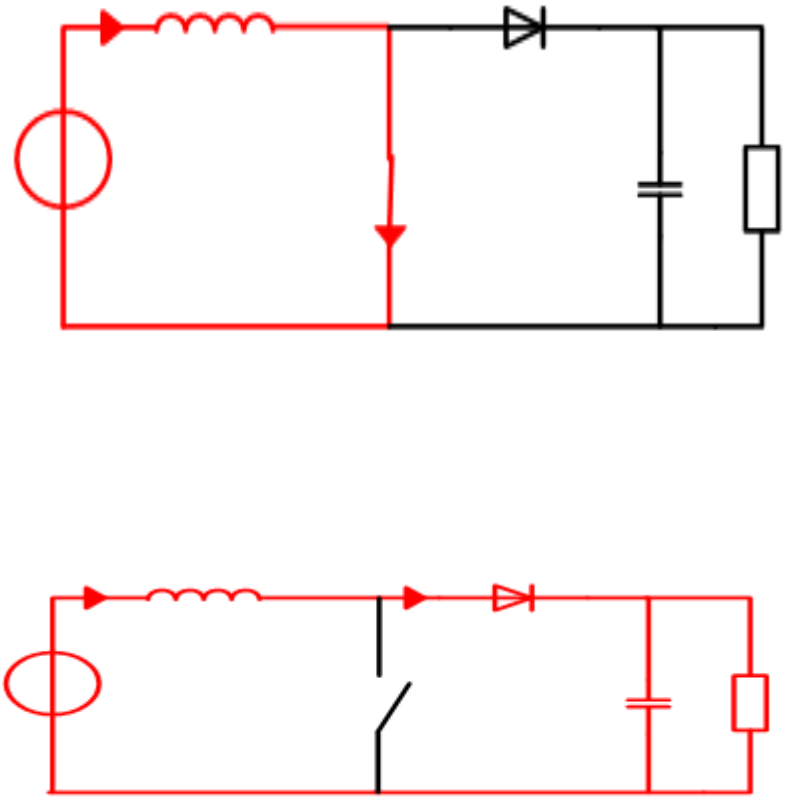

Figure 4.5: The two configurations of boost converter, depending on the state of the switch S

4.3.2.5 Continuous mode:

When a boost converter operates in continuous mode, the current through the inductor I_L never falls to zero. Figure 4.6 shows the typical waveforms of currents and voltages in a converter operating in this mode. The output voltage can be calculated as follows, in the case of an ideal converter i.e. using components with an ideal behaviour operating in steady conditions.

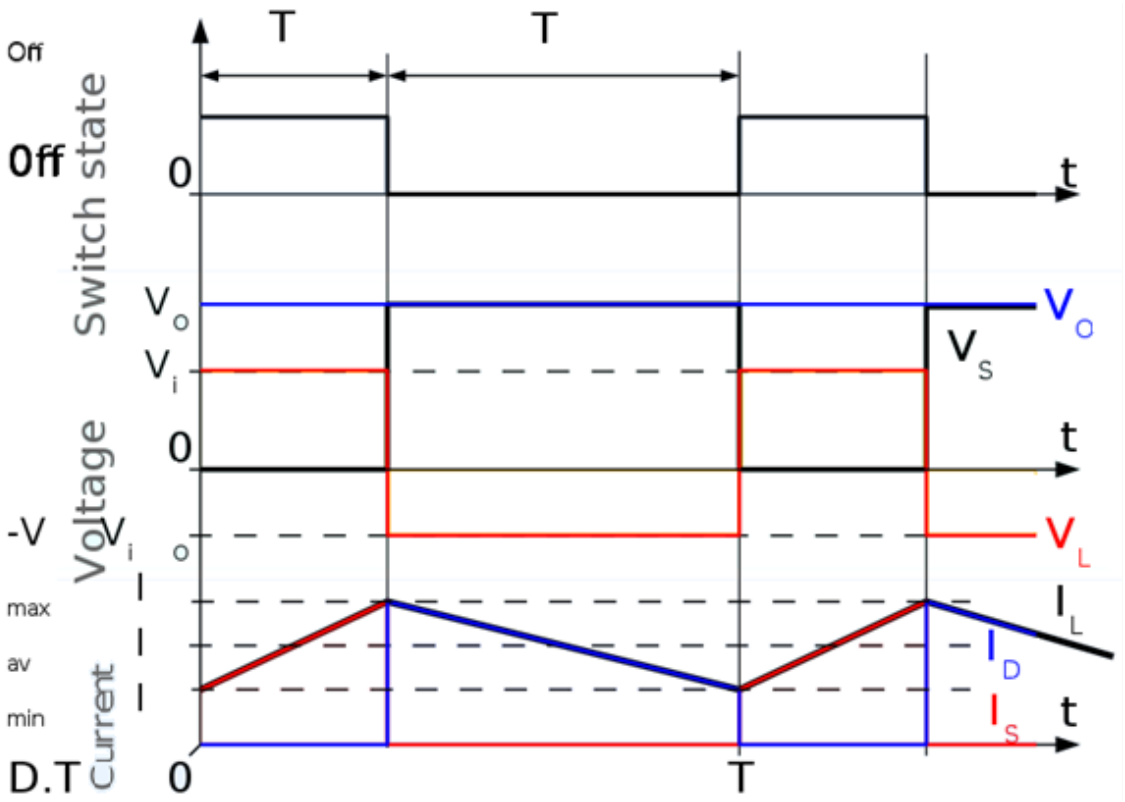

Figure 4.6: Waveforms of current and voltage in a boost converter operating in continuous mode

During the On-state, the switch S is closed, which makes the input voltage V_i appear across the inductor, which causes a change in current I_L flowing through the inductor during a time period t by the formula:

$$\frac{\Delta I_L}{\Delta t} = \frac{V_i}{L} \qquad (4.5)$$

At the end of the On-state, the increase of I_L is therefore:

$$\Delta I_{Lon} = \frac{1}{L}\int_0^{DT} V_i dt = \frac{DT}{L} V_i \qquad (4.6)$$

D is the duty cycle. It represents the fraction of the commutation period T during which the switch is ON. Therefore D ranges between 0 i.e., Switch is never on and 1 i.e., S is always on.

During the off-state, the switch S is open, so the inductor current flows through the load. If we consider zero voltage drops in the diode and capacitor large enough for its voltage to remain constant, the evolution of I_L is:

$$V_i - V_0 = L\frac{dI_L}{dt} \tag{4.7}$$

Therefore, the variation of I_L during the Off-period is:

$$\Delta I_{Loff} = \int_{DT}^{T} \frac{(V_i - V_0)dt}{L} = \frac{(V_i - V_0)(1-D)T}{L} \tag{4.8}$$

As we consider that the converter operates in steady state conditions, the amount of energy stored in each of its components has to be the same at the beginning and at the end of a commutation cycle. In particular, the energy stored in the inductor is given by:

$$E = \frac{1}{2}LI_L^2 \tag{4.9}$$

So, the inductor current has to be the same at the start and end of the commutation cycle. This means the overall change in the current i.e., the sum of the changes is zero.

$$\Delta I_{Lon} + \Delta I_{Loff} = 0 \tag{4.10}$$

Substituting ΔI_{LON} and ΔI_{LOFF} by their expressions yields:

$$\Delta I_{Lon} + \Delta I_{Loff} = \frac{V_i DT}{L} + \frac{(V_i - V_0)(1-D)T}{L} = 0 \tag{4.11}$$

This can be written as:

$$\frac{V_0}{V_i} = \frac{1}{1-D} \tag{4.12}$$

This in turn reveals the duty cycle to be:

$$D = 1 - \frac{V_i}{V_0} \tag{4.13}$$

The above expression shows that the output voltage is always higher than the input voltage as the duty cycle goes from 0 to 1 and that it increases with D, theoretically to infinity as D approaches 1. So, this converter is sometimes referred to as a step-up converter.

4.3.2.6 Discontinuous mode:

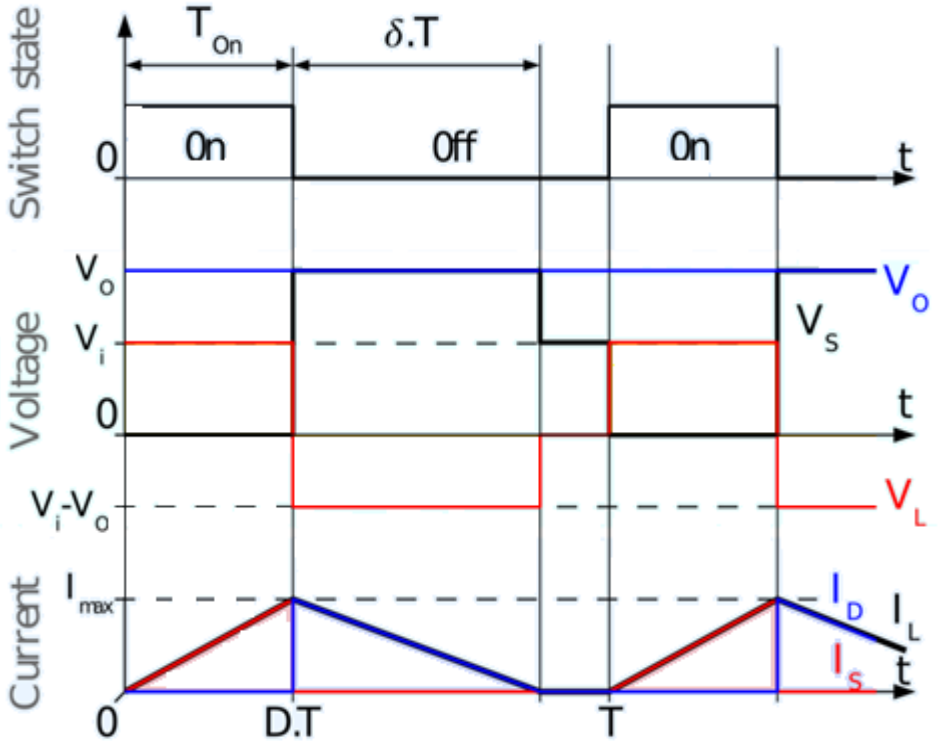

Figure 4.7: Waveforms of current and voltage in a boost converter operating in discontinuous mode.

If the ripple amplitude of the current is too high, the inductor may be completely discharged before the end of a whole commutation cycle. This commonly occurs under light loads. In this case, the current through the inductor falls to zero during part of the period as shown in figure 4.7. Although slight, the difference has a strong effect on the output voltage equation.

It can be calculated as follows:

As the inductor current at the beginning of the cycle is zero, its maximum value I_{LMax}at t=DT is given by

$$I_{LMax} = \frac{V_i DT}{L} \tag{4.14}$$

During the off-period, I_L falls to zero after δT:

$$I_{LMax} + \frac{(V_i - V_0)\delta T}{L} = 0 \tag{4.15}$$

Using the two previous equations, δ is:

$$\delta = \frac{V_i D}{V_0 - V_i} \tag{4.16}$$

The load current I_o is equal to the average diode current I_D From figure 4.4, the diode current is equal to the inductor current during the off-state. Therefore the output current can be written as:

$$I_0 = \bar{I_D} = \frac{I_{LMax}}{2}\delta \quad (4.17)$$

Replacing I_{Lmax} and δ by their respective expressions yields:

$$I_0 = \frac{V_i DT}{2L} \cdot \frac{V_i D}{V_0 - V_i} = \frac{V_i^2 D^2 T}{2L(V_0 - V_i)} \quad (4.18)$$

Therefore, the output voltage gain can be written as follows:

$$\frac{V_0}{V_i} = 1 + \frac{V_i D^2 T}{2LI_0} \quad (4.19)$$

Compared to the expression of the output voltage for the continuous mode, this expression is much more complicated. Furthermore, in discontinuous operation, the output voltage gain not only depends on the duty cycle, but also on the inductor value, the input voltage, the switching frequency and the output current.

4.3.3 Buck-Boost Converter:

A non-isolated (transformer-less) topology of the buck-boost converter is shown in Fig.4.8. The converter consists of dc input voltage source V_S, controlled switch S, inductor L, diode D, filter capacitor C, and load resistance R. With the switch on, the inductor current increases while the diode is maintained off. When the switch is turned off, the diode provides a path for the inductor current. Note the polarity of the diode that results in its current being drawn from the output.
The buck-boost converter waveforms are depicted in Fig.4.9. The condition of a zero volt-second product for the inductor in steady state yields

$$V_S DT = -V_O(1-D)T$$

Hence, the dc voltage transfer function of the buck-boost converter is

$$M_V = \frac{Vo}{Vs} = -\frac{D}{1-D}$$

The output voltage V_O is negative with respect to the ground. Its magnitude can be either greater or smaller (equal at D = 0.5) than the input voltage as the name of the converter implies.

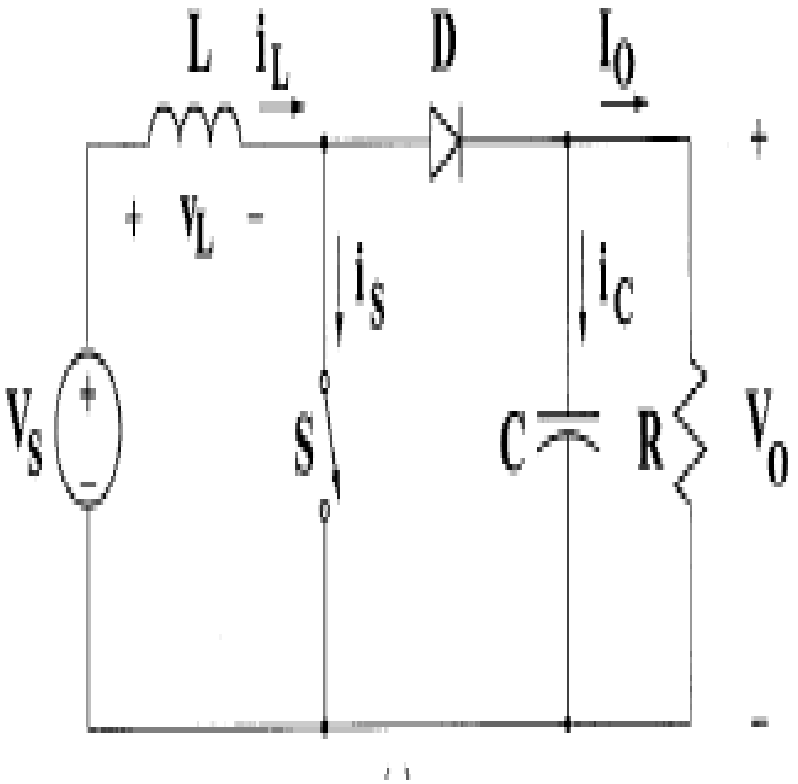

Figure 4.8: buck-boost converter

The value of the inductor that determines the boundary between the CCM and DCM is

$$L_b = \frac{(1-D)^2 R}{2f}$$

The structure of the output part of the converter is similar to that of the boost converter (reversed polarities are the only difference). Thus, the value of the filter capacitor can be obtained from Eq. (4.4).

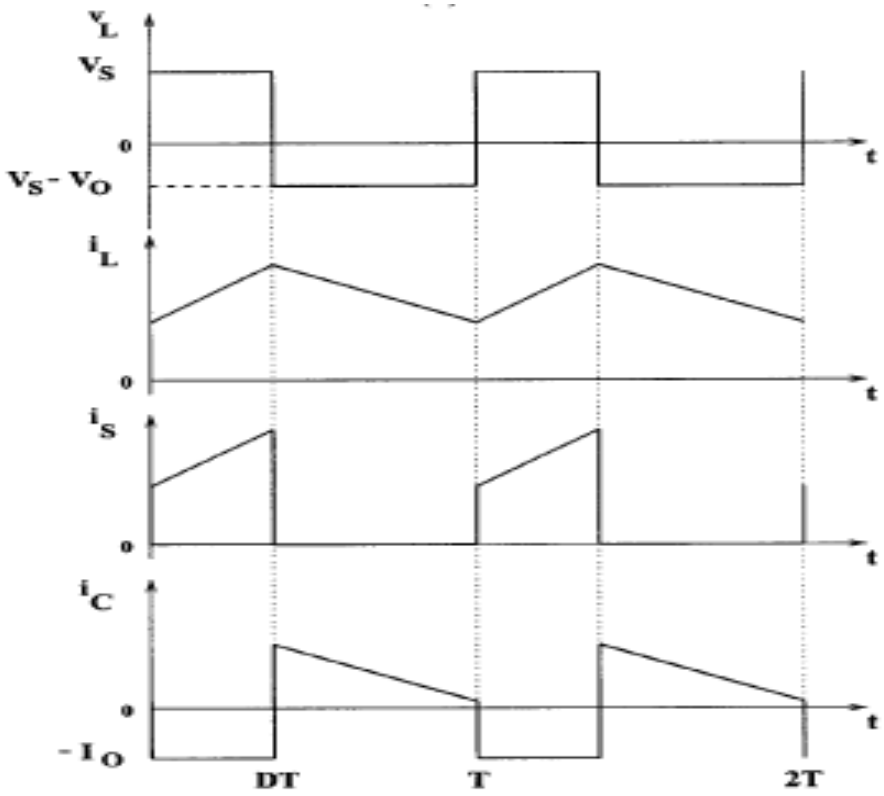

Figure 4.9: buck-boost converter waveform

CHAPTER 5

MAXIMUM POWER POINT TRACKER

5.1 PRINCIPLE OF MPPT

Maximum power point tracker (or MPPT) is a high efficiency DC to DC converter that presents an optimal electrical load to a solar panel or array and produces a voltage suitable for the load. PV cells have a single operating point where the values of the current (I) and Voltage (V) of the cell result in a maximum power output. These values correspond to a particular load resistance, which is equal to V/I as specified by Ohm's Law. A PV cell has an exponential relationship between current and voltage, and the maximum power point (MPP) occurs at the knee of the curve, where the resistance is equal to the negative of the differential resistance (V/I = -dV/dI). Maximum power point trackers utilize some type of control circuit or logic to search for this point and thus to allow the converter circuit to extract the maximum power available from a cell.

Traditional solar inverters perform MPPT for an entire array as a whole. In such systems the same current, dictated by the inverter, flows though all panels in the string. But because different panels have different IV curves, i.e. different MPPs (due to manufacturing tolerance, partial shading, etc.) this architecture means some panels will be performing below their MPP, resulting in the loss of energy.

Some companies (see power optimizer) are now placing peak power point converters into individual panels, allowing each to operate at peak efficiency despite uneven shading, soiling or electrical mismatch.

At night, an off-grid PV power system uses batteries to supply its loads. Although the battery pack voltage when fully charged may be close to the PV array's peak power point, this is unlikely to be true at sunrise when the battery is partially discharged. Charging may begin at a voltage considerably below the array peak power point, and a MPPT can resolve this mismatch. When the batteries in an off-grid system are full and PV production exceeds local loads, a MPPT can no longer operate the array at its peak power point as the excess power has nowhere to go. The MPPT must then shift the array operating point away from the peak power point until production exactly matches demand. (An alternative approach commonly used in spacecraft is to divert surplus PV power into a resistive load, allowing the array to operate continuously at its peak power point.)In a grid-tied photovoltaic system, the grid is essentially

a battery with near infinite capacity. The grid can always absorb surplus PV power, and it can cover shortfalls in PV production (e.g., at night). Batteries are thus needed only for protection from grid outages. The MPPT in a grid tied PV system will always operate the array at its peak power point unless the grid fails when the batteries are full and there are insufficient local loads. It would then have to back the array away from its peak power point as in the off-grid case (which it has temporarily become).

5.2 ALGORITHM OF PERTURB OBSERVE METHOD

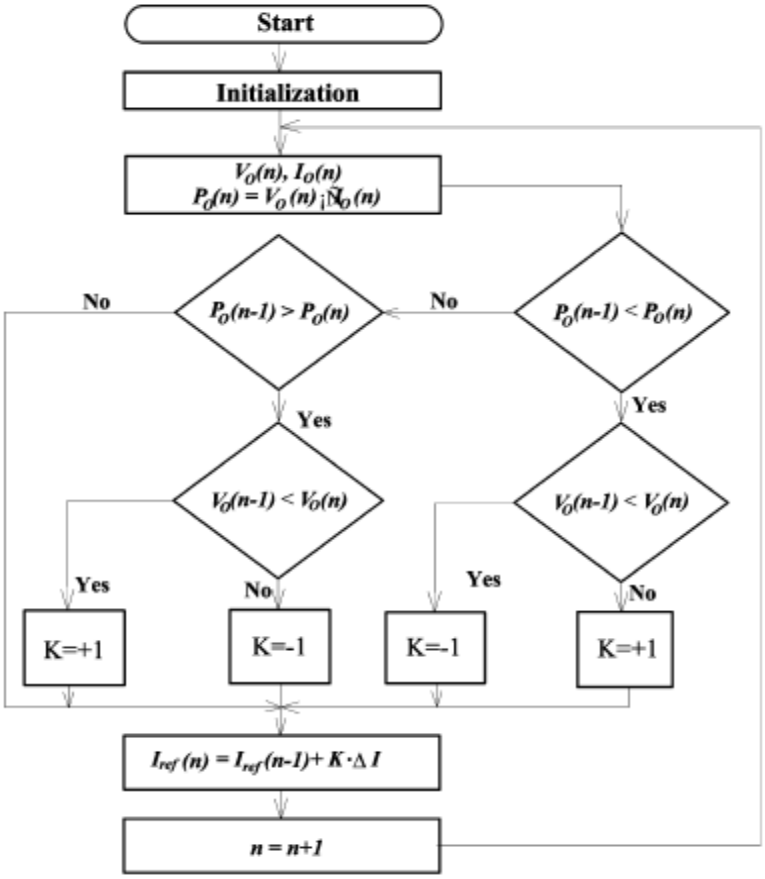

Fig .5.1 Flow chart of the MPPT algorithm with P&O method

By comparing the recent values of power and voltage with previous ones, the P&O method shown in the flow chart can determine the value of reference current to adjust the output power toward the maximum point.

MPPTs can be designed to drive an electric motor without a storage battery. They provide significant advantages, especially when starting a motor under load. This can require a starting current that is well above the short-circuit rating of the PV panel. A MPPT can step the panel's

relatively high voltage and low current down to the low voltage and high current needed to start the motor.

Once the motor is running and its current requirements have dropped, the MPPT will automatically increase the voltage to normal. In this application, the MPPT can be seen as an electrical analogue to the transmission in a car; the low gears provide extra torque to the wheels until the car is up to speed**.**

5.3 .HILL CLIMB SEARCH STRATEGY

Due to the similarities of the shape of the wind and PV array power curves, a similar maximum power point tracking scheme known as the hill climb search (HCS) strategy is often applied to these energy sources to extract maximum power. The HCS strategy perturbs the operating point of the system and observes the output. If the direction of the perturbation (e.g an increase or decrease in the output voltage of a PV array) results in a positive change in the output power, then the control algorithm will continue in the direction of the previous perturbation.

Conversely, if a negative change in the output power is observed, then the control algorithm will reverse the direction of the pervious perturbation step. In the case that the change in power is close to zero (within a specified range) then the algorithm will invoke no changes to the system operating point since it corresponds to the maximum power point (the peak of the power curves.

5.4 MPPT SCHEME OF β METHOD:

Fast MPPT scheme, called the "β" method , was suitably modified and used for the given application. The scheme is based on the observation that the value of an intermediate variable "β", defined only at MPP condition, varies with in a narrow band ($\beta_{max} - \beta_{min}$) as the MPP varies from PMPP(max) to PMPP(min) over the full isolation and temperature range (λ_{max}, T_{max} to λ_{min}, T_{min}), as shown in algorithm. β is a subset of β', which is applicable to any point on the P–V curve, including MPP.

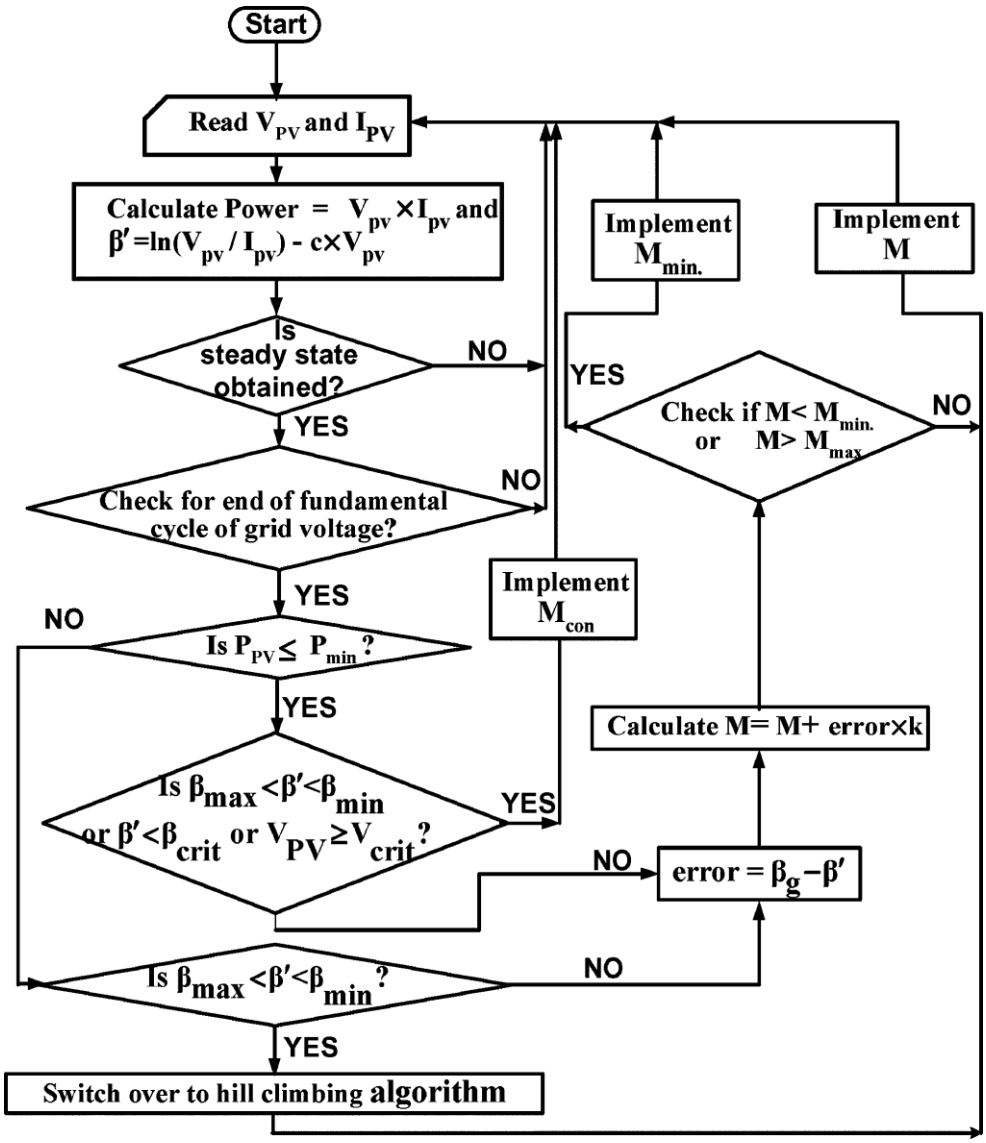

Fig 5.2. MPPT algorithm for β-method

β is obtained by using the MPP condition, $\partial P/dV = 0$ and is given by,

$$\beta = \ln(-I_o \times c) = \ln\frac{I_{pv}}{V_{pv}} - c \times V_{pv}$$

where I_o is the reverse saturation current of the diode. Therefore, by tracking β using large iterative steps, the operating point can be quickly brought into a narrow band of MPP. Also, controlling "β" indirectly controls the operating voltage (OV) of the PV array, which helps in balancing the power across capacitor C_{PV}.

It is important to note that problems may arise during the low insolation phase when the generated PV power is very small and the value of "M", as computed by the MPP algorithm, is small. Under such conditions, as FC continues to feed the deficit power, this will result in a voltage increase across C_{PV} due to imbalance between the input and output power. This may lead to shifting of OV of the PV array toward the OCC. The array will remain at OCC even when high or normal insolation is restored and the system will continue to draw the required

power from FC. To avoid such a situation, the algorithm has been suitably modified to ensure that the PV array voltage is always less than or equal to a critical voltage (V_{crit}), which is less than the PV array's V_{OC}. Whenever the array voltage goes beyond V_{crit} (which occurs only when the power drawn from the FC is not fed into the grid due to the low value of M) and array power is less than the minimum power P_{min}, the modulation index is set to a fixed value (M_{con}) by the algorithm. This ensures that $V_{PV} \leq V_{crit}$.

5.5. INCREMENTAL CONDUCTANCE METHOD

This method consists in using the slope of the derivative of the current with respect to the voltage in order to reach the maximum power point.

What advantage does MPPT give in the real world that depends on the array, their climate, and their seasonal load pattern? It gives us an effective current boost only when the Vpp is more than about 1V higher than the battery voltage. In hot weather, this may not be the case unless the batteries are low in charge. In cold weather however, the Vpp can rise to 18V. If ther energy use is greatest in the winter (typical in most homes) and the have cold winter weather, then the can gain a substantial boost in energy when the need it the most.

Here is an example of MPPT action on a cold winter day:

Outside temperature: 20°F (-7°C) Wind is blowing a bit, so the PV cell temperature rises to only around 32°F (0°C). Vpp = 18V Batteries are a bit low, and loads are on, so battery voltage = 12.0

Ratio of Vpp to battery voltage is 18:12 = 1.5:1

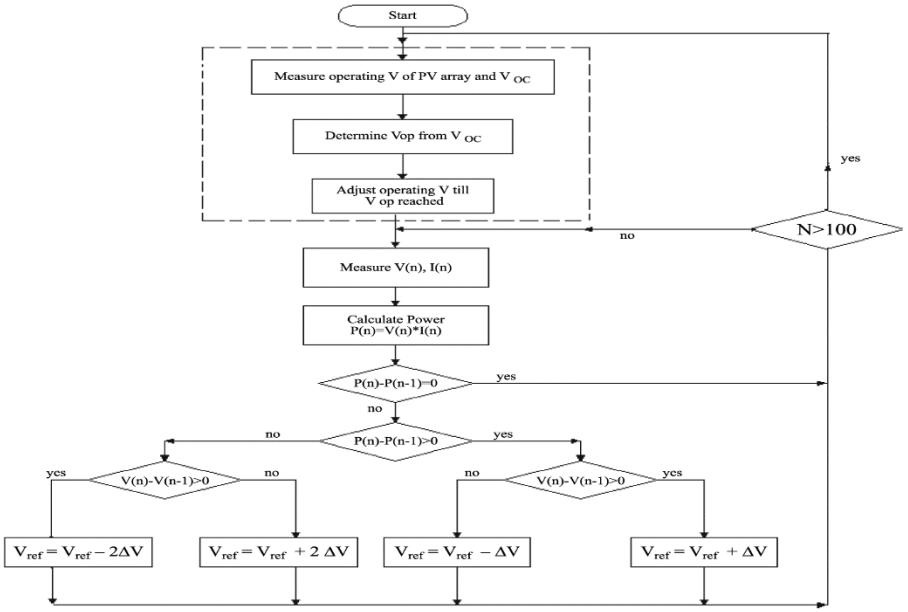

Fig 5.3: Incremental Conductance Method Algorithm

Under these conditions, a theoretically perfect MPPT (with no voltage drop in the array circuit) would deliver a 50% increase in charge current. In reality, there are losses in the conversion just as there is friction in a car's transmission. Reports from the field indicate that increases of 20 to 30% are typically observed.Both the wind turbine and the photovoltaic array must be adjusted to operate at their point of maximum power. Many different maximum power point tracking (MPPT) algorithms like perturbation observation method, incremental conductance method have been developed and widely used for such systems. The perturbation observation method is adopted in this paper for both the wind turbine and the photovoltaic array for it simplicity and accuracy. The algorithm starts by choosing an initial reference rotor speed for the wind turbine and an initial reference voltage for the photovoltaic array. The corresponding output powers of the two systems are measured. If this power does not correspond to their maximum powers, then their initial reference values are incremented or decremented by one step. If this adjustment leads to an increase in their output powers then the next adjustment is made in the same direction and vice-versa. The above steps are repeated till the maximum power points of the wind turbine and photovoltaic array are reached.

5.6 Fractional Open Circuit Voltage (FOCV) MPPT

Fractional open-circuit voltage algorithm is based on V_PV (the maximum voltage at the output of the PV array) which is said as maximum power point voltage and mentioned as Vmpp. This algorithm works on the base of relation between Vmpp and VOC [7]. The maximum peak power is a constant voltage of open-circuit voltage it is given by Eq. (5.1)

$$V_{mpp} = k_v . V_{OC} \qquad 5.1$$

where kv is a constant which is between 0.7 and 0.8 depending on the PV cell characteristic measured based on maximum power point voltage and open-circuit voltage. The fig. 5.4 shows the flow chart of the algorithm [8].

$$V_{mpp} = k_v . V_{OC}$$

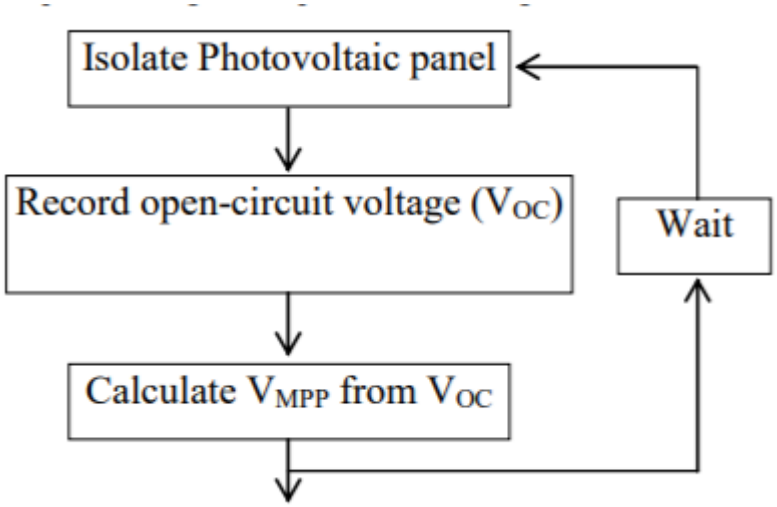

Fig.5.4 Flowchart of open-circuit voltage method

The voltage generated by the diode in the cell is approximately 75% of the open-circuit voltage. Once the maximum power point is approximated, closed loop control in the PV array boost converter is used to get the desired output voltage at the PV array [9]. The open-circuit voltage taken from the PV array output, and is measured without connecting it to the load. The maximum power point voltage is approximated by taking the reference voltage in the algorithm.

CHAPTER-6

MODELLING OF CASE STUDY

6.1 PROPOSED SYSTEM

The system layout investigated in this paper is shown in Fig. 6.1. It consists of a solar PV connected through a DC/DC boost converter where the MPPT algorithm receives the current (Ipv)and voltage (Vpv) values of the solar PV and outputs the duty cycle that switches the boost converter in order to extract maximum power from the solar PV. On the other hand, the charging and discharging of the battery is performed by the battery charge controller through the bidirectional buck-boost converter, whereby the parameters considered are battery current (Ib)and voltage at the DC bus (Vdc) to ensure that the voltage at the DC bus is kept constant. The system is designed to operate 750V at a DC bus voltage of as will be described later in this work. Moreover, considering the needs of loads in rural areas, the solar PV is designed to generate up to 200kW. Solar PV as the main source of power operates at Maximum Power Point (MPP) while the battery ESS complements the entire system by charging or discharging in order to balance power supplied to the DC and AC loads. The wind power system is connected at the AC bus and appropriate inverter control is imposed to maintain the voltage and frequency at PCC constant

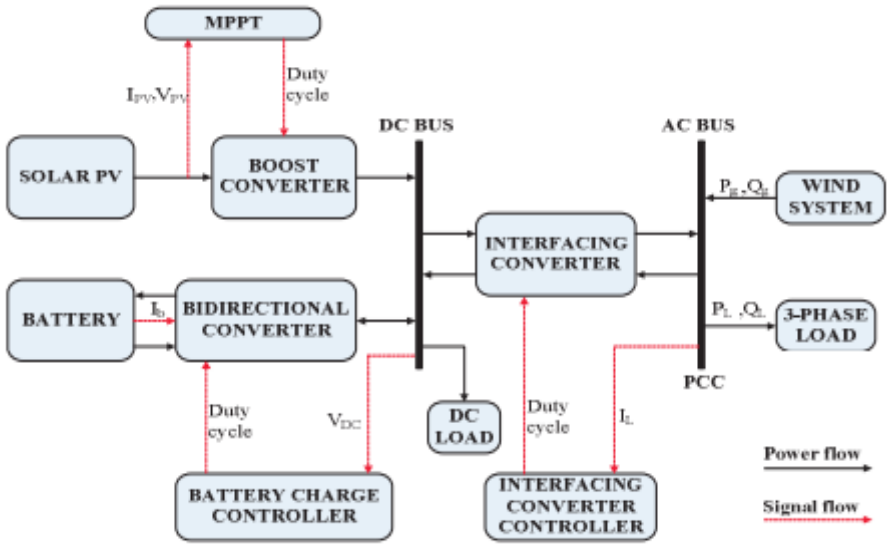

Fig. 6.1: Block diagram of the proposed system

6.1.1 PV CELL MODELLING

The photovoltaic effect is the basic principle that makes a PV cell convert incident solar radiation (sunlight) into electricity. Solar radiation, which constitutes infrared heat waves and visible light waves, when getting incident on a photovoltaic cell get absorbed, reflected, or even go right through [12]. During this phenomenon, the light that is absorbed develops useful electricity. Each category of the photovoltaic panel has its own distinct attributes correlating to the atmospheric parameters like temperature and solar irradiance. These cells are either connected in parallel, series or series-parallel array combinations that might depend upon the end-user application. If they are connected in series, the net voltage gets added up and in a parallel combination, the overall current delivered is summed up based on the number of cells or PV array connected, and while in series-parallel combination, required voltage and current levels can be achieved.

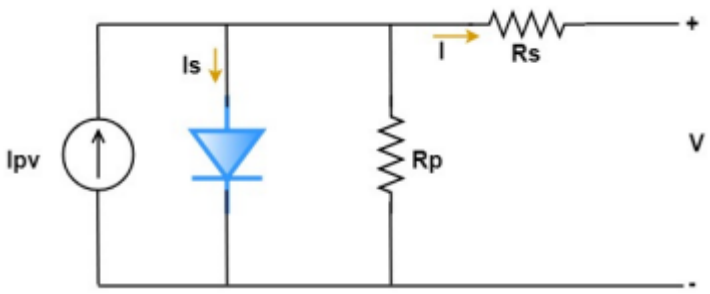

Fig. 6.2. One Diode model of Solar Photo Voltaic system

The solar cell is modeled based on the IV characteristics of a solar PV panel, given in equation 6.1 [13].

$$I = I_{pv} - I_s \left(exp\left(\frac{q(V + IR_s}{N_s kTa} \right) - 1 \right) - \frac{V + R_s I}{R_p} \qquad 6.1$$

Where: Ipv : Photo Voltaic Current (A) Is : Reverse Saturation Current (A) q : Charge of Electron (1.602176 × 10−19C) k : Boltzmann's constant (1.3806 × 10−23J/K) a : Ideality constant for Diode Rs : Resistance in Series with the cell (Ω) Rp : Resistance in Parallel with the cell (Ω) Ns : Number of Cells in series T : Atmospheric Temperature (K) The equivalent one diode model of the solar PV cell is given in fig. 6.1.

6.1.2 Rotor Side Converter Control Strategy (RSC) of DFIG

Field oriented control is adopted to control the RSC to maintain voltage and frequency constant despite of the load change or variation of the wind speed. The dynamic model of the DFIG in the synchronous reference frame is used as in [20], [21]. The stator flux linkage (λ_s) is aligned along the d-q axis of the synchronous d-q reference frame, Then, the d-axis and q-axis components of the stator flux linkage will be as follows:

$$\lambda_{ds} = \lambda_s \, , \; \lambda_{qs} = 0. \qquad 6.2$$

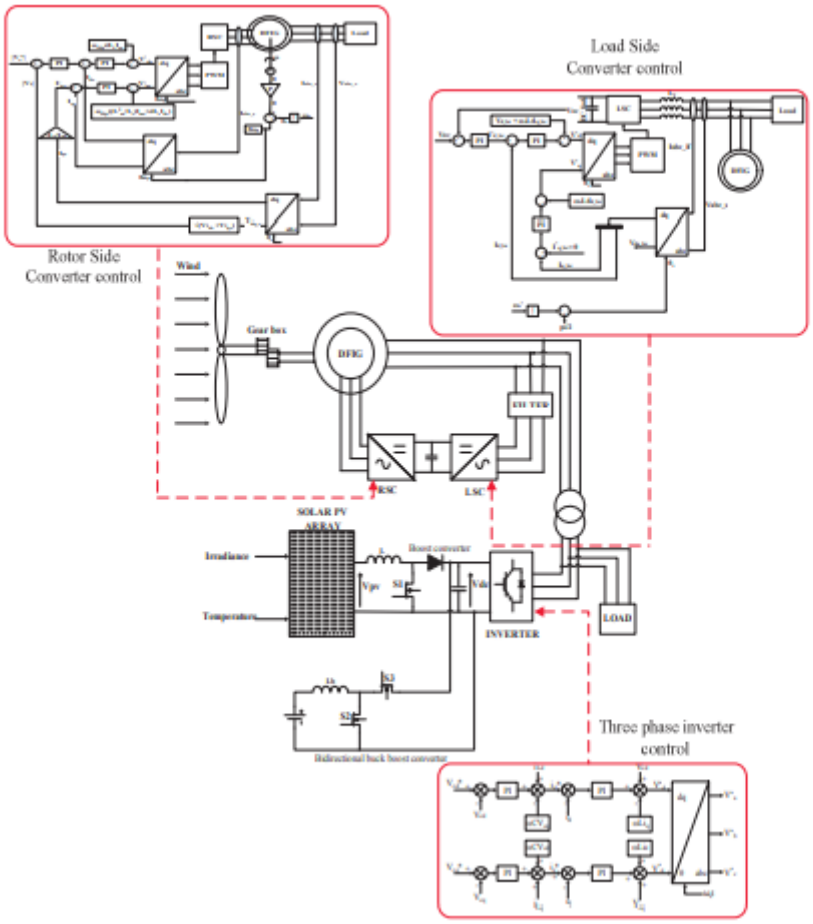

Fig. 6.3: Hybrid solar PV-wind system

The d-axis and q-axis components of the rotor flux, λ_{dr} and λ_{dq} can be expressed as:

$$\lambda_{dr} = L_r I_{dr} \qquad 6.3$$

$$\lambda_{qr} = L_r\left(1 - \frac{L_m^2}{L_s L_r}\right) I_{qr} \quad 6.4$$

whereL_r, $L_s$and $L_m$are the rotor, stator and mutual inductances. Then, the d-axis and q-axis rotor voltages equations of DFIG will be as follows:

$$V_{dr} = R_r I_{dr} + pL_r I_{dr} - \omega_{slip} L_r \sigma I_{qr} \quad 6.5$$

$$V_{qr} = R_r I_{qr} + pL_r I_{qr} + \omega_{slip} L_r I_{dr} \quad 6.6$$

Where, $\sigma = 1 - \frac{L_m^2}{L_s L_r}$ and $\omega_{slip} = \omega_s - \omega_r$.

6.1.3 Interfacing Converter Control of Hybrid System

The main objective of controlling this converter is to maintain the voltage and the system frequency at the Point of Common Coupling (PCC) constant as portrayed in Figs. 1 and 3. The circuit dynamics in d-q reference frame will be:

$$C\frac{dV_{cd}}{dt} - \omega C V_{cq} = i_d - i_{Ld} \quad 6.7$$

$$C\frac{dV_{cq}}{dt} + \omega C V_{cd} = i_q - i_{Lq} \quad 6.8$$

$$L\frac{di_d}{dt} - \omega L i_q = V_d - V_{cd} \quad 6.9$$

$$L\frac{di_q}{dt} - \omega L i_d = V_q - V_{cq} \quad 6.10$$

where, V_{cd} and $V_{cq}$are the capacitor voltages in d and q axis, i_d and i_q are the converter currents in d and q axis, i_{Ld} and i_{lq} are the load currents in d and q axis.

6.14 Hybrid Solar PV-Wind System

Then, the hybrid solar PV-wind system together with the associated control schemes is depicted in Fig. 6.3.

CHAPTER-7

MATLAB AND SIMULINK

7.1: MATLAB Introduction:

MATLAB is an abnormal state specialized figuring language and intelligent condition for calculation advancement, information perception, information examination, and numeric calculation. Utilizing the MATLAB item, you can take care of specialized processing issues quicker than with customary programming languages, for example, C, C++, and FORTRAN.

MATLAB is utilized in wide scope of uses, including sign and picture preparing, correspondences, control configuration, test and estimation, monetary demonstrating and examination, and computational science. Extra tool kits (accumulations of exceptional reason MATLAB capacities, accessible independently) stretch out the MATLAB condition to take care of specific classes of issues in these submission library.

MATLAB gives various highlights to exposure and allocation your work. Synchronize your MATLAB code with different applications,languages and appropriate your MATLAB calculations and applications.

7.1.1: KEY FEATURES:

- High-level language for specialized processing.
- Development condition for overseeing code, records, and information.
- Interactive instruments for iterative investigation, structure, and critical thinking.
- Mathematical capacities for direct polynomial math, measurements, Fourier investigation, sifting, enhancement, and numerical combination.
- Functions for incorporating MATLAB based calculations with outside applications and languages, for example, C, C++, FORTRAN, Java, COM, and Microsoft Exceed expectations.

7.2: SIMULINK Introduction:

Simulink is a situation for multi-space recreation and Model-Based Plan for dynamic and implanted frameworks. It gives an intuitive graphical condition and an adjustable arrangement of square libraries that let you configuration, reproduce, execute, and test an assortment of time-differing frameworks, including correspondences, controls, signal handling, video preparing, and picture handling.

Extra items stretch out Simulink programming to numerous displaying areas, just as give apparatuses to plan, execution, and confirmation and approval undertakings.

7.2.1: KEY FEATURES:

- Extensive and expandable libraries of predefined blocks.
- Interactive graphical supervisor for amassing and overseeing natural square outlines.
- Ability to oversee complex structures by portioning models into progressive systems of plan segments.
- Model Pilgrim to explore, makes, arranges, and look through all sign, parameters, properties, and produced code related with your model.
- Application programming interfaces (APIs) that let you associate with other recreation programs and fuse manually written code.
- Embedded MATLAB™ Capacity blocks for bringing MATLAB calculations into Simulink and installed framework usage.
- Simulation modes (Typical, Quickening agent, and Fast Quickening agent) for running reenactments interpretively or at assembled C-code speeds utilizing fixed-or variable-advance solvers.
- Graphical debugger and profiler to look at reproduction results and after that analyze execution and startling conduct in your plan.
- Full access to MATLAB for examining and imagining results, redoing the displaying condition, and characterizing sign, parameter, and test information.
- Model examination and diagnostics devices to guarantee model consistency and distinguish demonstrating blunders.

7.2.2 BLOCK DIAGRAM:

A Simulink square layout is a pictorial model of a dynamic structure. It contains a great deal of pictures, called squares, interconnected by lines. Each square addresses a simple novel system that makes a yield either reliably (a consistent square) or at unequivocal concentrations in time (a discrete square). The lines address relationship of square commitments to square yields. Each square in a square layout is a case of a specific kind of square. The sort of the square chooses the association between a square's yields and its wellsprings of data, states, and time. A square diagram can contain any number of instances of a square expected to show a structure. Squares address simple novel systems that Simulink acknowledges how to impersonate. A square incorporates in any event one of the going with:

A lot of wellsprings of information,

A lot of states, and

A lot of yields.

A square's yield is a part of time and the square's wellsprings of data and states (accepting any). The specific limit that relates a square's respect its wellsprings of data, states, and time depends upon the kind of square of which the square is a precedent. Diligent Versus discrete Blocks Simulink's standard square set fuses steady squares and discrete squares. Steady squares respond always to constantly advancing data. Discrete squares, then again, respond to changes in data exactly at crucial results of a fixed interval called the square's model time. Discrete squares hold their yield consistent between dynamic model time hits. Each discrete square joins a model time parameter that empowers you to show its precedent rate. The Simulink squares can be perpetual or discrete, dependent upon whether they are driven by reliable or discrete squares. A square that can be either discrete or relentless is said to have a specific precedent rate. The certain model time is steady if any of the square's information sources are relentless. The specific model time is proportionate to the most short data test time if all the data test times are fundamental results of the most constrained time. Something different, the data test time is identical to the significant model time of the data sources, where the pivotal precedent time of a great deal of test times is described as the best number divisor of the plan of test times.

7.2.3 SIMULINK BLOCK LIBRARIES:

Simulink can on the other hand shading code a square graph to demonstrate the model occasions of squares it has, e.g., dim (relentless), maroon (enduring), yellow (mutt), red (snappiest discrete, and so on. The square contains square name, image, and square library that contain the square, the inspiration driving the square.

Simulink deals with its squares into square libraries according to their lead:

•The Sources library contains hinders that produce signals.

• The Sinks library contains obstructs that show or create square yield.

• The Discrete library contains obstructs that depict discrete-time parts.

• The Ceaseless library contains obstructs that portray direct limits.

• The Math library contains obstructs that delineate general science limits.

• The Capacities and Tables library contains obstructs that depict general limits and table investigate exercises.

• The Nonlinear library contains obstructs that depict nonlinear limits.

• The Signal and Frameworks library contains obstructs that grant multiplexing and demultiplexing, execute outside data/yield, pass data to various bits of the model, and perform various limits.

• The Subsystems library contains obstructs for making various types of subsystems.

• The Square sets and Toolboxes library contains the Additional things square library of specific squares.

7.2.4 SUB SYSTEMS:

Simulink licenses to show a confusing structure as a huge amount of interconnected subsystems which is all tended to by a square diagram. We make a subsystem utilizing Simulink's Subsystem square and the Simulink model chief. We can acquaint subsystems with subsystems with any criticalness to make dynamic models. We can make restrictively executed subsystems that are executed precisely when headway happens on a starting or connecting with data.

7.3 SIMULINK BLOCKS USED IN THE SIMULATION:

1. Three - phase source

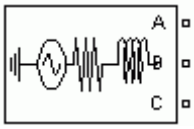

Purpose: Implement three-phase source with internal R-L impedance.

Description: The Three-Phase Source square executes a sensible three-arrange voltage source with internal R-L impedance. The three voltage sources are related in Y with a fair affiliation that can be inside grounded or made accessible. You can demonstrate the source inside deterrent and inductance either honestly by entering R and L regards or by suggestion by deciding the source inductive short out measurement and X/R extent.

2.In port

Purpose: Provide a link to an external input and for linearization.

Description: In ports are the associations from the outside world into a structure. Inside a subsystem discourage, there is an in port contrasting with every data port on the square. A sign that grounds at a data port on a subsystem shut streams out of the relating in port inside that square. The imports inside a subsystem square ought to be numbered consecutively, starting with1.

3. Out port

Purpose: Accumulates a path to an external output and for the linearization.

Description: The Out port square gives a component to marking a framework's yields. In a subsystem, yield ports relate to yields on the subsystem square.

4. Subsystem

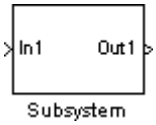

Purpose: Group blocks into a subsystem

Description: Subsystem blocks speak to one framework inside another framework. Any arrangement of blocks and lines can be changed over to a Subsystem obstruct with the Gathering order on the choices menu. The Gathering order expels every single chosen object from the dynamic window and replaces them inside a Subsystem square. This new square, when opened, redisplays the majority of the assembled goals.

5. Gain

Purpose: Multiply its input by a constant.

Description: The Gain square executes Y=KU, where Y is the yield, U is the information, and K is the predefined gain. The Increase square shows scalar expansion data entered as factor or a predictable. The square demonstrates the substance as it appears in the trade box.

6. Scope

Purpose: Display signals during simulation.

Description: While the entertainment is running, the Extension square demonstrates the yield of the square driving it. Opening an expansion square conveys a degree window. The title of this window organizes the name of the square.

7. Voltage measurement

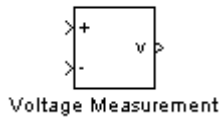

Purpose: Measure a voltage in a circuit

Description: The Voltage Measurement block is utilized to quantify the immediate voltage between two electric hubs. The yield is a Simulink signal that can be utilized by other Simulink blocks.

8. Bus bar

Purpose: Implement a labeled network node

Description: The Bus Bar block is utilized to interconnect segments. It permits various electrical square yields and contributions to be associated together.

11. Current measurement

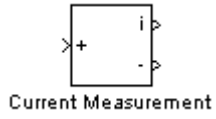

Purpose: Measure a current in a circuit

Description: The Current Measurement block is utilized to quantify the momentary flow streaming in any electrical square or association line. The principal yield gives a Simulink signal that can be utilized by other Simulink blocks.

12. Distributed parameters line

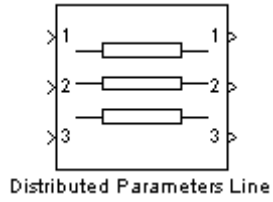

Purpose: Executed a N-phase by lumped losses are provided in distributed parameter transmission line model.

Description: The Distributed Parameter Line block implements an N-phase distributed parameter line model with lumped losses.

13. Linear transformer

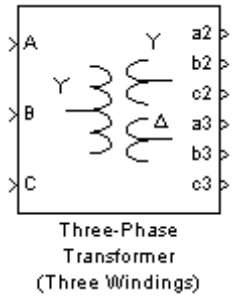

Purpose: Implement a two- or three-winding linear transformer

Description: The Linear Transformer block model appeared underneath comprises of three coupled windings twisted on a similar center

CHAPTER-8

SIMULATION RESULTS

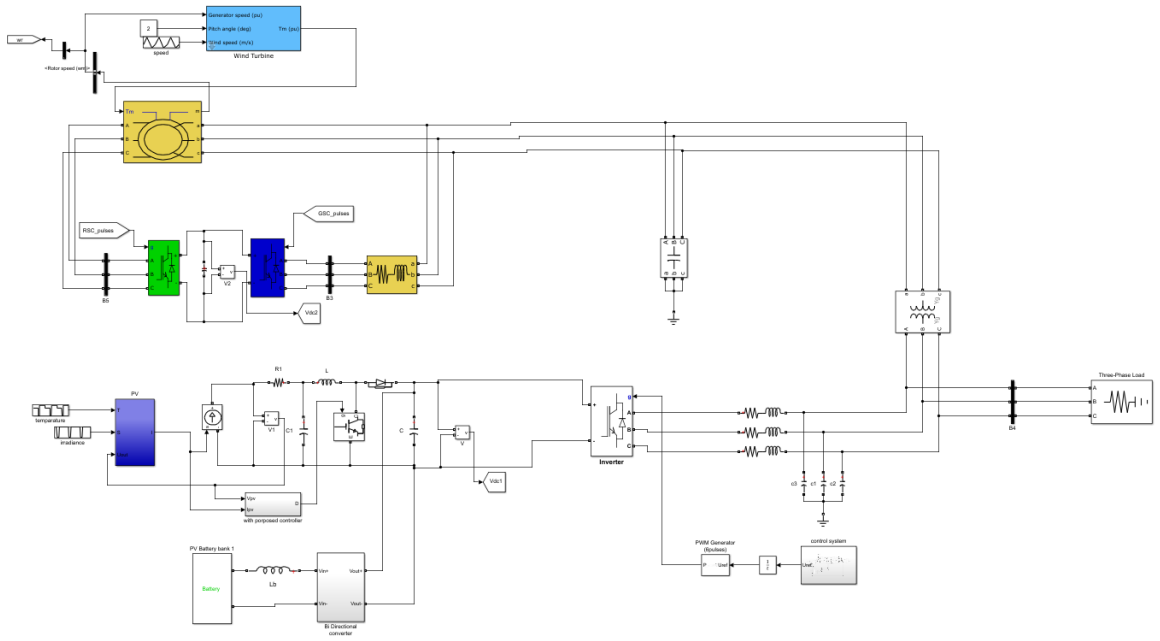

Fig. 8.1 MATLAB/Simulink model of Proposed System

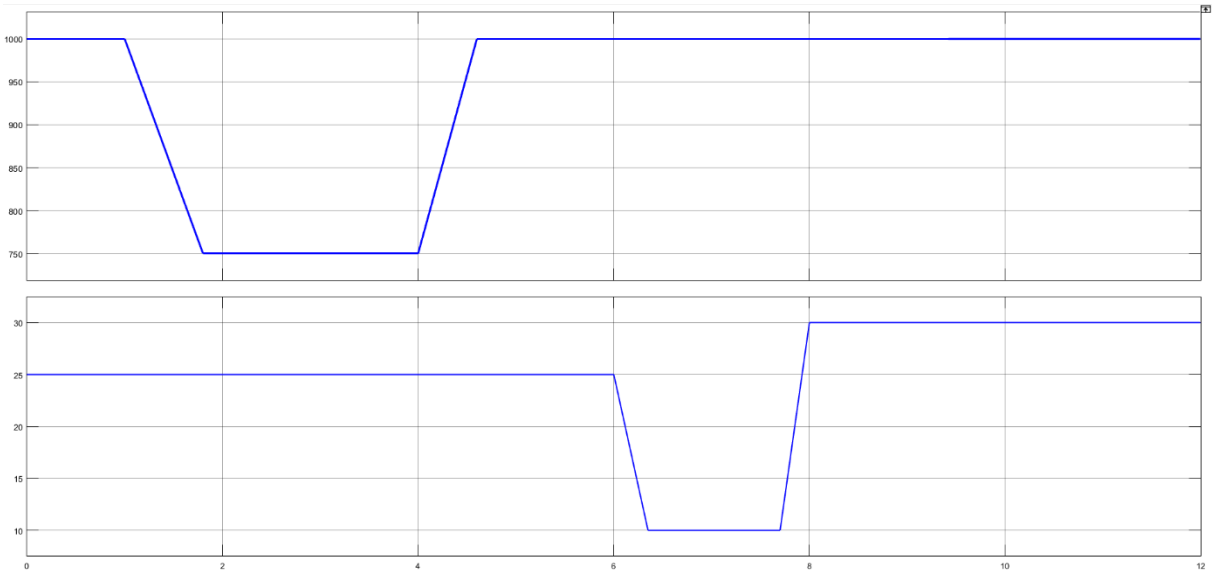

Fig. 8.2: Variable irradiance and temperature waveforms

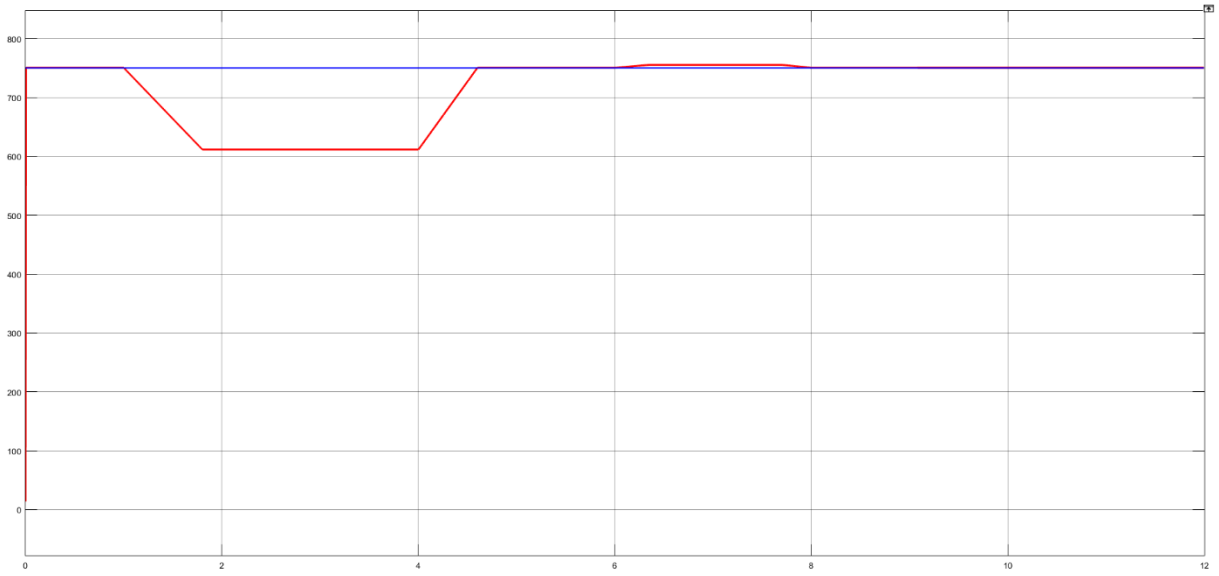

Fig. 8.3: DC bus voltages response with Solar PV alone on variable irradiance and temperature without controller action.

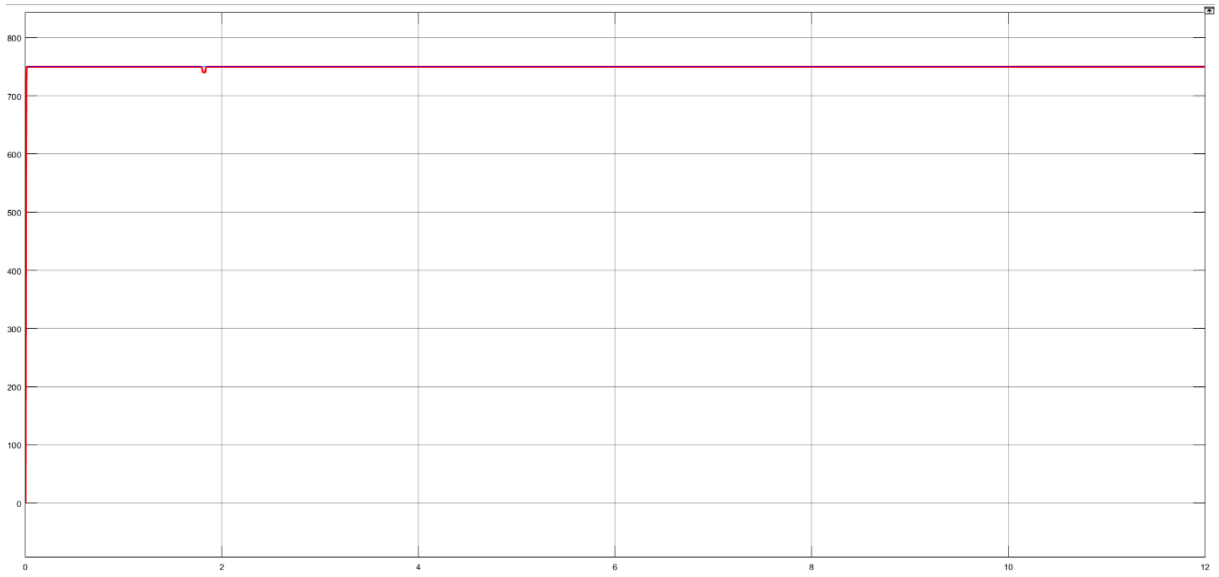

Fig.8.4: DC bus voltage response with solar PV alone on variable irradiance and temperature with proposed controller actions

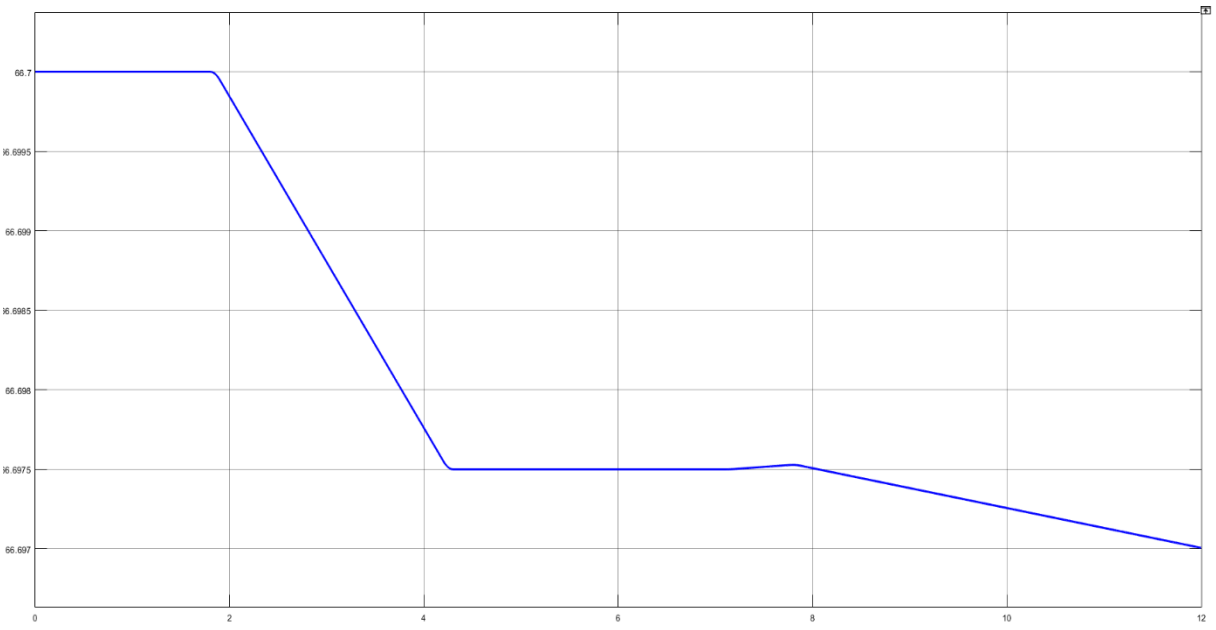

Fig.8.5 : BESS SOC response with solar PV on variable irradiance and temperature

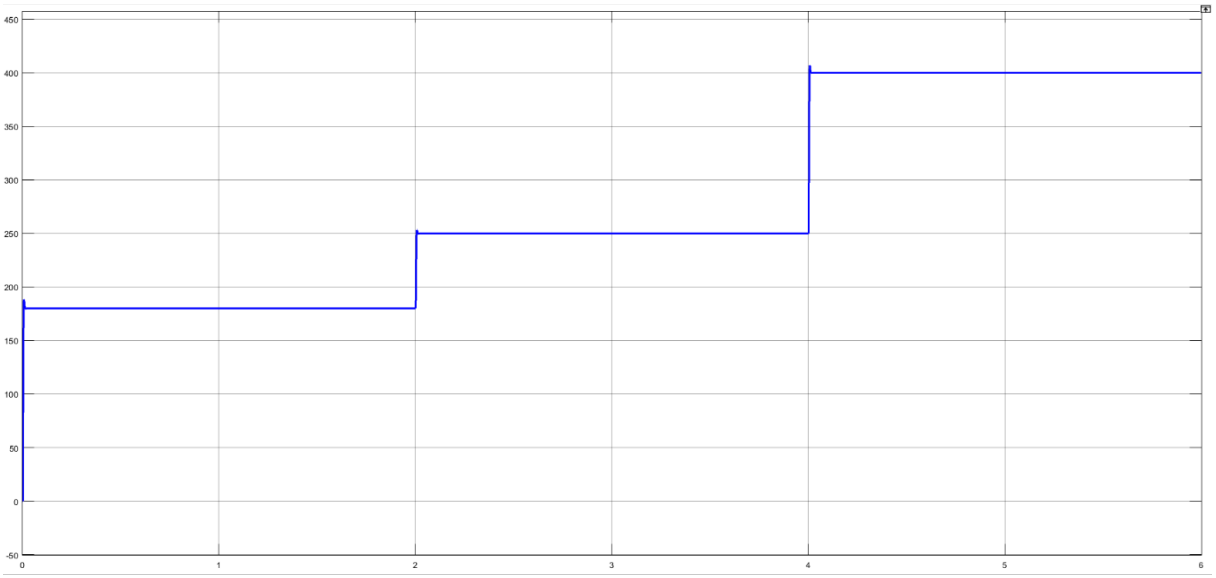

Fig. 8.6: DC link current response with solar PV-BESS on step load change with proposed controller action.

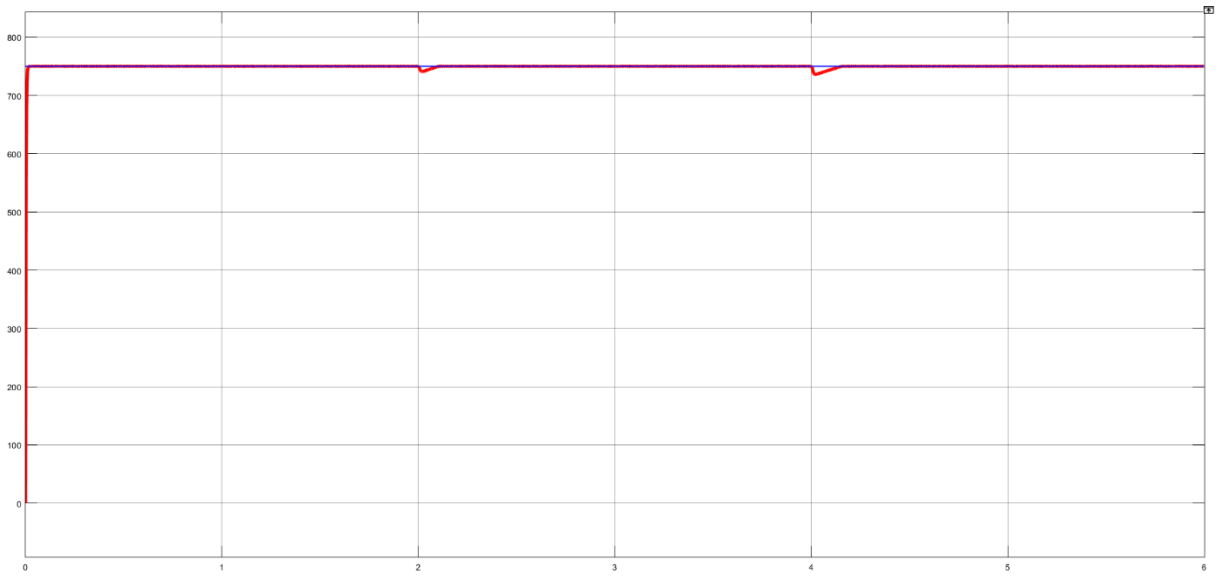

Fig. 8.7 : Response of DC bus voltage with solar PV-BESS on step load changes with proposed controller action

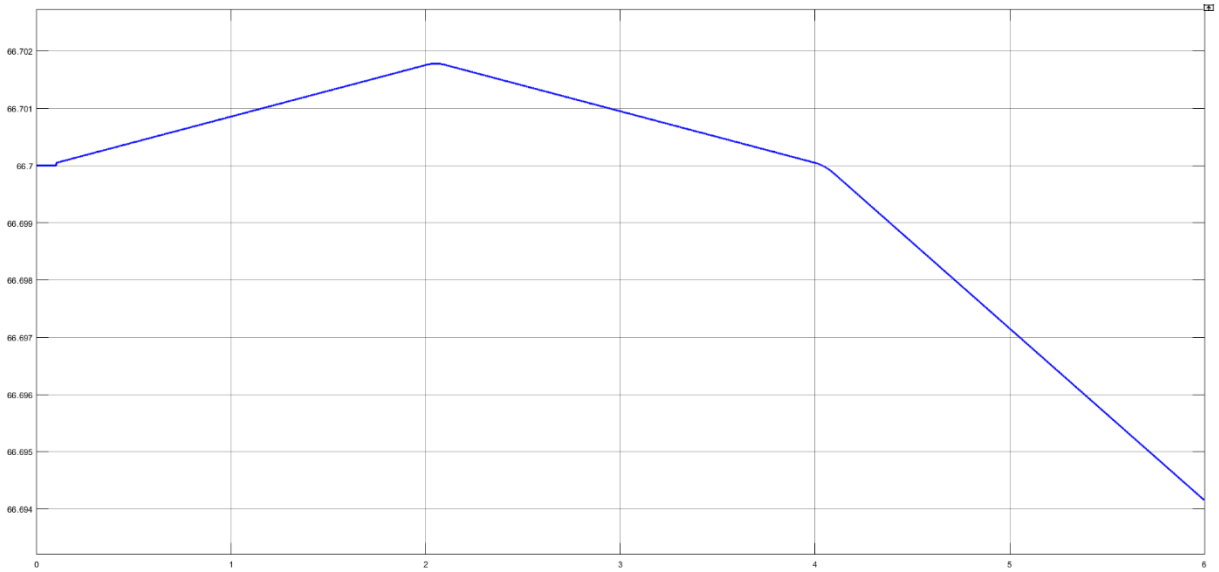

Fig. 8.8: BESS SOC response with solar PV-BESS on step load changes with proposed controller action

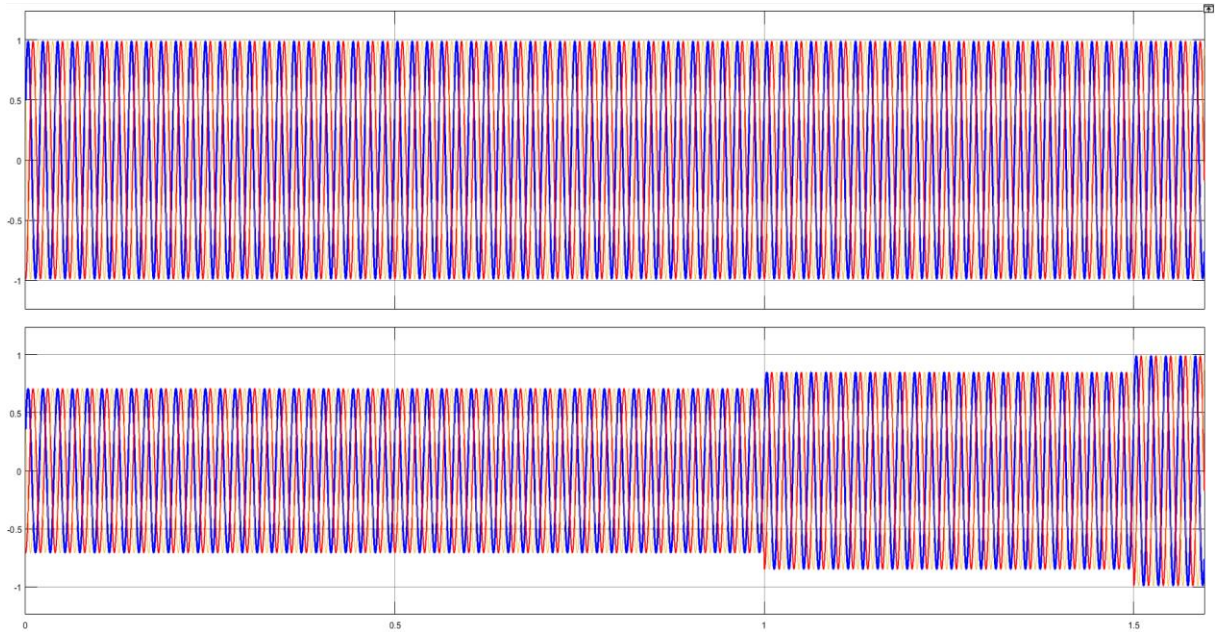

Fig. 8.9: Voltage and current waveforms of the DFIG-based WECS on varying load with proposed controller action.

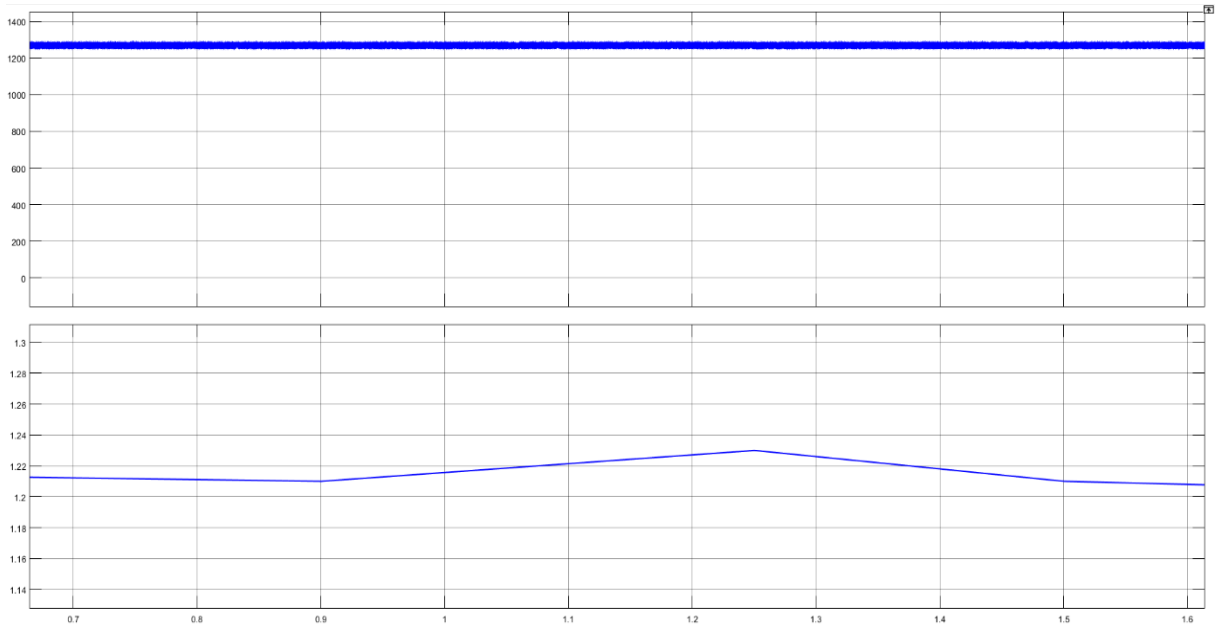

Fig. 8.10: DFIG-based WECS responses on load variations.

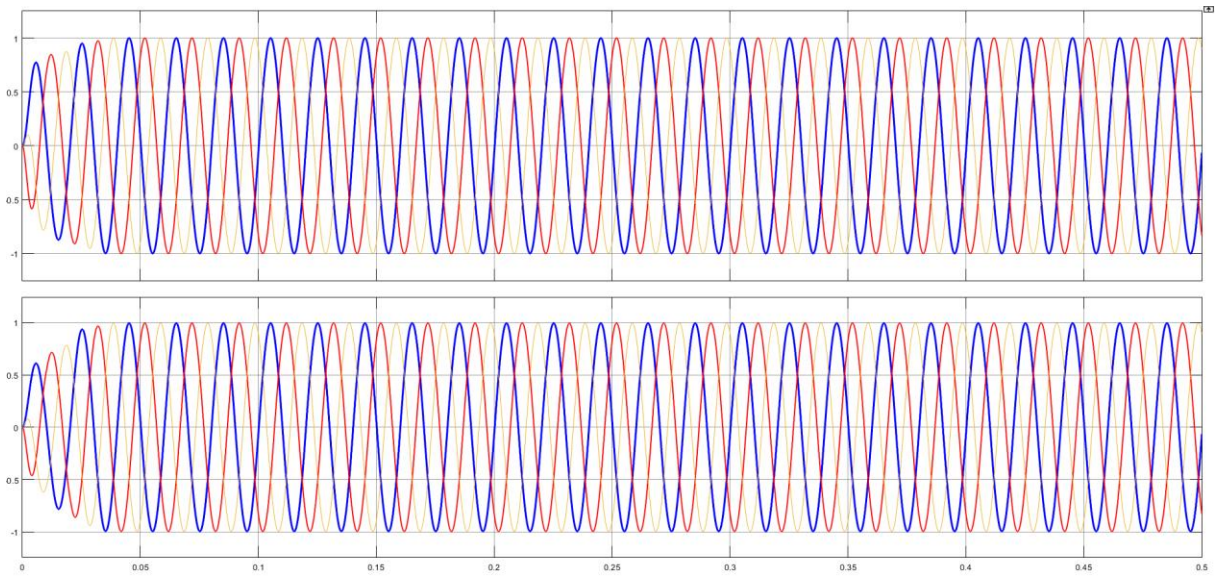

Fig. 8.11: Voltage at PCC and current waveforms of the overall hybrid solar PV-wind with BESS system.

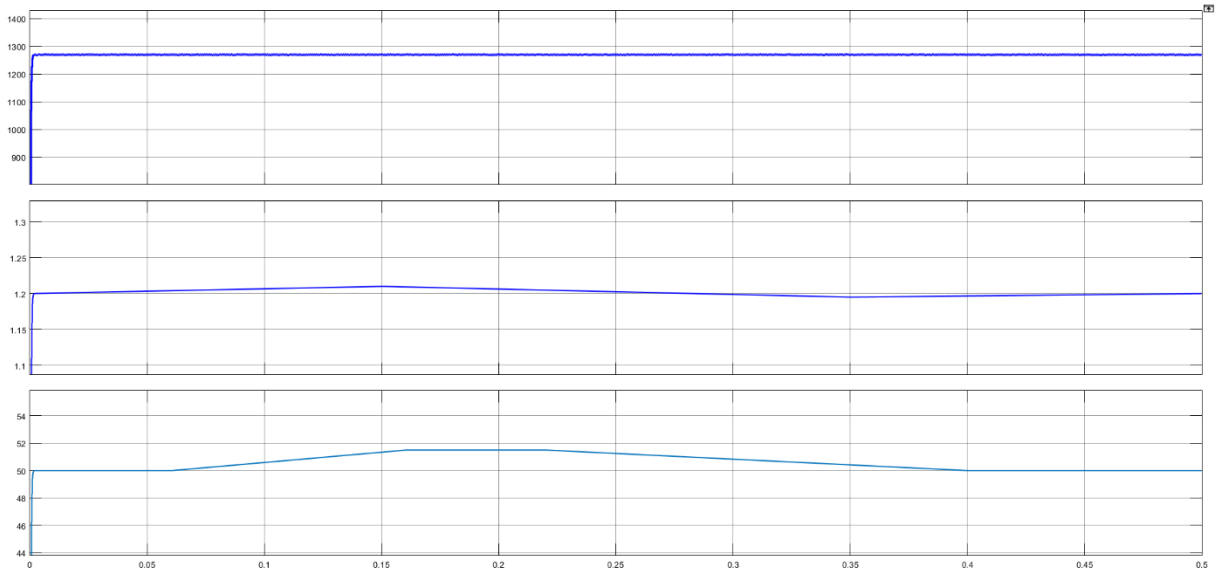

Fig. 8.12: DC link voltage, rotor speed and frequency responses of the overall hybrid solar PV-wind with BESS system.

CONCLUSION

In this paper, modelling and coordination control of hybrid solar PV-wind system for rural electrification applications is has been presented. The proposed control scheme maintains the system frequency and voltage at the PCC notwithstanding the load variations. It has been confirmed that proper optimization of the ESS highly reduced investment cost of renewable systems that can expedite rural electrification. Performance of the system has been validated through simulations carried out in MATLAB/Simulink platform where different scenarios were successfully tested and demonstrated excellent results.

REFERENCES

[1] J. C. L. Júnior, T. Sousa, R. da Silva Benedito, F. B. M. Trigoso, and D O. G. Medina, "Application of Battery Energy Storage System in Photovoltaic Power Plants Connected to the Distribution Grid," In 2019 IEEE PES Innovative Smart Grid Technologies Conf.,-Latin America (ISGT Latin America), pp. 1-6.

[2] M. Muralikrishna and V. Lakshminarayana, "Hybrid (Solar and Wind) Energy Systems for Rural Electrification," ARPN J. Eng. App. Sci., vol. 3, no. 5, 2008.

[3] S. Teske, T. Morris, and K. Nagrath, "100% Renewable Energy for Tanzania–Access to renewable and affordable energy for all within one generation", Institute for Sustainable Futures, University of Technology Sydney, Sydney, Dec. 2017.

[4] A. Aly, et al., "Barriers to Large-scale Solar Power in Tanzania," Energy Sustain. Dev., vol. 48, pp. 43-58, Feb. 2019.

[5] S. Venkataraman, C. Ziesler, P. Johnson, and S. Van Kempen "Integrated wind, solar, and energy storage: Designing plants with a better generation profile and lower overall cost," IEEE Power Energy Mag., vol. 16, no. 3, pp. 74-83, Apr. 2018.

[6] I. Elsayed, I. Nassar, and F. Mostafa, "Optimization and economic evaluation of small scale hybrid solar/wind power for remote areas in Egypt," 2017 Nineteenth International Middle East Power Systems Conf. (MEPCON), pp. 1-6.

[7] A. H. Fathima and K. Palanisamy, "Optimization in microgrids with hybrid energy systems–A review," Renew. Sustain. Energy Rev., vol. 45, pp. 431-446, May 2015.

[8] S. Bahramirad and H. Daneshi, "Optimal sizing of smart grid storage management system in a microgrid," 2012 IEEE PES Innov. Smart Grid Tech. (ISGT), pp. 1-7.

[9] X. Xiong, K. T. Chi, and X. Ruan, "Bifurcation analysis and experimental study of a multi-operating-mode photovoltaic-battery hybrid power system," IEEE J Em. Sel. Top. C., vol. 5, no. 3, pp. 316- 325, Sep. 2015.

[10] H. Bevrani and S. Shokoohi, "An intelligent droop control for simultaneous voltage and frequency regulation in islanded microgrids," IEEE Trans. Smart Grid, vol. 4, no. 3, pp. 1505-1513, May 2013.

[11] A. Micallef, M. Apap, C. Spiteri-Staines, J. M. Guerrero and J. C. Vasquez, "Reactive power sharing and voltage harmonic distortion compensation of droop controlled single phase islanded microgrids," IEEE Trans. Smart Grid, vol. 5, no. 3, pp. 1149-1158, Feb. 2014.

[12] J. Hu, J. Zhu, D. G. Dorrell, and J. M. Guerrero, "Virtual flux droop method—A new control strategy of inverters in microgrids," IEEE Trans. Power Electron., vol. 29, no. 9, pp. 4704-4711, Sep. 2014.

[13] X. Y. Wang, D. M. Vilathgamuwa, and S. S. Choi, "Determination of battery storage capacity in energy buffer for wind farm" IEEE Trans. Energy Convers., vol. 23, no. 3, pp. 868-878, May 2008.

[14] S. J. Chiang, K. T. Chang, and C. Y. Yen, "Residential photovoltaic energy storage system," IEEE Trans. Ind. Electron., vol. 45, no. 3, pp. 385-394, Jun. 1998.

[15] C. Venu, Y. Riffonneau, S. Bacha, and Y. Baghzouz, "Battery storage system sizing in distribution feeders with distributed photovoltaic systems," 2009 IEEE Bucharest Power Tech, pp. 1-5.

[16] H. T. Le and T. Q. Nguyen, "Sizing energy storage systems for wind power firming: An analytical approach and a cost-benefit analysis," 2008 IEEE Power and Energy Society General Meeting-Conversion and Delivery of Electrical Energy in the 21st Century, pp. 1-8.

[17] J. K. Kaldellis, D. Zafirakis, and E. Kondili, "Optimum sizing of photovoltaic-energy storage systems for autonomous small islands," Int J Elec. Power., vol. 32, no. 1, pp. 24-36, Jan. 2010.

[18] Z. Zhao, "Optimal energy management for microgrids," Ph.D. dissertation, Clemson Univ. Clemson, USA, 2012.

[19] S. Bahramirad, W. Reder, and A. Khodaei, "Reliability-constrained optimal sizing of energy storage system in a microgrid," IEEE Trans. Smart Grid, vol. 3, no. 4, pp. 2056-2062, Dec. 2012.

[20] R. Pena, J. C. Clare, and G. M. Asher, "A doubly fed induction generator using back-to-back PWM converters supplying an isolated load from a variable speed wind turbine," IEE Proc.-Electric Power Applications 143, no. 5, pp. 380-387, Sep. 1996.

[21] G. Abad, J. Lopez, M. A. Rodriguez, L. Morroyo, G. Iwanski, Doubly fedinduction machine: modeling and control for wind energy generation, Hoboken: Wiley, 2011.